UNIKASSEL
VERSITÄT

Optimization Strategies for Electric Vehicle Charging Schedules

By

Erkki Juha Matti Rautiainen

A Thesis Submitted to
the Faculty of Engineering at
Cairo University and Kassel University
In Partial Fulfillment of the
Requirements for the Degree of
Master of Science
in
RENEWABLE ENERGY AND ENERGY EFFICIENCY

University of Kassel - Kassel, Germany
Faculty of Engineering, University of Cairo - Giza, Egypt

May 2015

Optimization Strategies for Electric Vehicle Charging Schedules

By

Erkki Juha Matti Rautiainen

A Thesis Submitted to
the Faculty of Engineering at
Cairo University and Kassel University
In Partial Fulfillment of the
Requirements for the Degree of
Master of Science
in
RENEWABLE ENERGY AND ENERGY EFFICIENCY

Under the Supervision of

Prof. Dr. -sc.techn. Dirk Dahlhaus
Kassel University, Germany

Prof. Dr. Mohamed El Sobki (Jr.)
Cairo University, Egypt

M.Sc. Chenjie Ma
Fraunhofer Institute for Wind Energy and
Energy System Technology (IWES), Kassel, Germany

University of Kassel - Kassel, Germany
Faculty of Engineering, University of Cairo - Giza, Egypt

May 2015

Optimization Strategies for Electric Vehicle Charging Schedules

By

Erkki Juha Matti Rautiainen

A Thesis Submitted to
the Faculty of Engineering at
Cairo University and Kassel University
In Partial Fulfillment of the
Requirements for the Degree of
Master of Science
in
RENEWABLE ENERGY AND ENERGY EFFICIENCY

Approved by the Examining Committee:

Prof. Dr. Mohamed El Sobki (Jr.) Faculty of Engineering, Cairo University	Prof. Dr. Adel Khalil Faculty of Engineering, Cairo University
Prof. Dr. Hafez El-Salamawy Faculty of Engineering, Cairo University	Prof. Dr. -sc.techn. Dirk Dahlhaus University of Kassel

University of Kassel - Kassel, Germany
Faculty of Engineering, University of Cairo - Giza, Egypt

May 2015

Declaration

„To the best of my knowledge I do hereby declare that this thesis is my own work. It has not been submitted in any form of another degree or diploma to any other university or other institution of education. Information derived from the published or unpublished work of others has been acknowledged in the text and a list of references is given.“

Erkki Juha Matti Rautiainen

Signature

Place and Date

Acknowledgements

It is my pleasure to thank all those who made this thesis possible. I would like to express my deepest appreciation to Fraunhofer IWES, Germany for hosting the topic of my thesis. It has been a pleasure to work with my supervisor, M.Sc. Chenjie Ma from the Distribution System Operation at Fraunhofer IWES, Kassel, whom I would like to thank for his cooperation and constructive criticism. I would also like to express my gratitude to Dr. Frank Marten from the Distribution System Operation at Fraunhofer IWES, Kassel for his valuable insights throughout the work.

It gives me great pleasure in acknowledging the support of the master program administration team for their true cooperation and support. I'm privileged to have carried out this Master Thesis under the supervision of Univ.-Prof. Dr.-sc.techn. Dirk Dahlhaus, Dean of the Faculty of Electrical Engineering and Computer Science at Kassel University. He has been a great source of inspiration for me during my master's thesis.

I express my gratitude for to the Federal Ministry for Economic Affairs and Energy of Germany for funding the project „SIEM: Systemintegration Elektromobilität“ (BMWI, Grant no. 0325402) under which this master thesis was carried out. Realistic driving profiles of Germany from the „Mobility in Germany 2008“ dataset are used in this work. This dataset is property of the Federal Ministry of Transport, Building and Urban Development (BMVI) and was provided for non-commercial research in SIEM on 14th October 2014. I am grateful to the Federal Ministry of Transport, Building and Urban Development (BMVI) for providing this useful information.

My appreciation also goes to my fellow interns and master thesis students at Fraunhofer IWES, Kassel for their support as well as to all of my friends back home (Finland) and in Germany. Last but not least in importance, my family who colors my life. I owe all of my success to their kind and warm encouragements.

Abstract

As the penetration rate of the Electric Vehicles (EV) increases, their uncontrolled charging could cause undervoltages and network congestions in the electric network. To mitigate these impacts, the controlled charging of the EVs has been investigated by earlier publications. However, the controlled charging cannot be easily implemented as it involves multiple stakeholders having individual interests. The project „SIEM: Systemintegration Elektromobilität“ funded by the Federal Ministry for Economic Affairs and Energy in Germany is carried out at Fraunhofer IWES, Kassel to investigate the EV charging strategies in order to avoid the aforementioned electric network impacts caused by increased EV charging.

In this thesis, a new realistic charging strategy that accounts for the different stakeholder requirements is developed. In the new charging strategy, the Distribution System Operator (DSO) and the charging service provider are treated as separate entities. The DSO will not be burdened by the EV information and the charging service provider is aware only of the EV locations in the electric network. Furthermore, an uncontrolled charging scenario and three existing charging strategies are derived from the earlier publications. They are used to compare and evaluate the new charging strategy. The simulations are carried out in a MATLAB-Simulink environment. The simulation model consists a realistic electric network model and an EV model equipped with synthetically generated household load profiles and realistic EV user behaviors. The EV user behaviors are derived from the surveyed dataset collected by the project „Mobility in Germany 2008“ commissioned by the Federal Ministry for Transport, Building and Urban development of Germany. Moreover, to enable the on-line simulations, the strategies are implemented using moving window optimization and the electric network model is simulated by a real-time transient stability simulator named ePHASORsim, developed by Opal-RT.

The results indicate that the new charging strategy can result in considerable charging cost savings for the EV users in comparison with the uncontrolled charging scenario. Also the network losses, and the costs of the network losses are considerably reduced by the new charging strategy. In comparison with the uncontrolled charging scenario, the main competing strategy, which combines the DSO and the charging service provider into one entity results in higher network loss reductions than the new charging strategy. However, the new charging strategy results in higher charging cost reductions. Also in many cases, the costs for the network losses are comparable to the main competing strategy. Additionally, the multi charging service provider scenarios are simulated by having the new charging strategy always as the second strategy. In comparison to the charging strategies which have more emphasis on electric network constraints, the combination with the new charging strategy produces lesser reduction in network losses. However, the corresponding costs for the network losses are smaller. Also in these combinations, the new charging strategy reduce the total charging costs and charging interruptions. The results indicate the new charging strategy has potential for further development.

Key words— electric vehicle, charging, scheduling, optimisation.

Contents

List of Tables

List of Figures

Nomenclature

Abbreviations

ABS	Aggregator Based Strategy
BS	Base load Scenario
DoD	Depth of Discharge
DBS	DSO Based Strategy
SoC	State of Charge
SBS	System Based Strategy
CBS	Communication Based Strategy
UCS	Uncontrolled Charging Scenario
AC	Alternating Current
Ah	Ampere-hour
CS	Charging Scheduling
DC	Direct Current
EPEX	European Power Exchange
EV	Electric vehicle
h	Hour
km	Kilometer
kVA	Kilovoltampere
kW	Kilowatt
kWh	Kilowatthour
LV	Low voltage
RE	Renewable energy
V2G	Vehicle-to-Grid

Mathematical Symbols

α	Charger loss coefficient
P_{comp}	Active power for constant comparison point
Q_{comp}	Reactive power for constant comparison point
$\Delta\delta$	Voltage angle difference
$\Delta\mathbb{I}$	Complex current difference
$\mathbf{\Delta P}$	Active power difference
$\mathbf{\Delta Q}$	Reactive power difference
$\mathbf{\Delta V}$	Voltage magnitude difference
$\Delta\mathbb{V}$	Complex voltage difference
$\mathbb{J}^{-1}$	Inverse of the Jacobian matrix
βbatt	Battery capacity [Ah]
cP_{EV}	Cumulative peak power due to EV charging
$\mathbb{Y}_{\text{bus}}$	Bus admittance matrix
$\Delta\mathbb{I}_{\text{EV},n,n}$	Current effects of the nth EV
$\Delta\mathbb{I}_{\text{hh},h,\tau}$	Current effects of the hth household at time step τ
$\Delta\tau$	Length of a time step

$\Delta\mathbb{V}_{\mathrm{EV},n,n}$	Voltage effects of the nth EV
$\Delta\mathbb{V}_{\mathrm{hh},h,\tau}$	Voltage effects of the hth household at time step τ
P_{EV}	EV charging power rate
$\mathbf{P}_{\mathrm{hh},h,\tau}$	Power demand of the hth household at time step τ
M	Set of nodes in the electric network
N	Set of nodes with an EV connected
H	Set of nodes with a household connected
L	Set of nodes where a line is ending
T	Set of time steps within an optimization window
γ_{batt}	EV battery capacity [kWh]
ρ	Number of cells in parallel
ξ	Number of cells in series
$\boldsymbol{\Upsilon}$	Vector of EV user constraints
$\boldsymbol{\Theta}$	Vector of electric network constraints
$\boldsymbol{\Gamma}$	Vector of power capacity constraints for the CBS
$\mathbf{C}_{\tau}$	Electricity price at time step τ
C_{P}	Cost penalty factor
E_{km}	Energy consumption per km
$\sigma_{\mathrm{EV},n}$	Distance driven by the nth EV
$\mathbf{DoD}_{\mathrm{EV},n}$	DoD of the nth EV battery
$\mathbf{E}_{\mathrm{EV},n}$	Energy demand of the nth EV
$\mathbf{SoC}_{\mathrm{EV},n}$	SoC of the nth EV battery
F	Set of main feeders in the electric network
I_{DC}	DC current
$\mathbb{I}_{\mathrm{ref},l}$	Constant reference current of the lth line
$\mathbb{V}_{\mathrm{ref},m}$	Constant reference voltage of the mth node
$\mathbf{I}_{max}$	Maximum current limit
V_{max}	Maximum voltage limit
V_{min}	Minimum voltage limit
P_{AC}	AC power
P_{DC}	DC power
P_{P}	Power penalty factor
R_{batt}	Internal resistance of the battery
η	Battery resistance coefficient
SoC_{full}	SoC for full battery
U_{batt}	Battery voltage
ζ	Battery voltage coefficient
$\mathbf{P}_{f,\tau}$	Power limit of the fth feeder at time step τ
$\mathbf{P}_{\mathrm{tot},\tau}$	Global power capacity at time step τ
P_{max}	Maximum annual load
$\mathbf{x}_{n,\tau}$	Charging schedule of the nth EV at time step τ

Chapter 1

Introduction

As part of the German energy transition „Energiewende“ the transportation sector is moving towards sustainable mobility. In Germany, the transportation sector contribute approximately one fifth of CO_2 emissions [1], while EU wide it is responsible for a quarter of total emissions. In both cases, the transportation sector is almost entirely dependent on conventional energy. In reducing the transportation sector's emissions, Electric Vehicles (EV) are an important part of the solution. They can mitigate the tail pipe emissions, are quieter and also three times more energy efficient when compared with vehicles powered by internal combustion engines [2]. This has been noted in Germany's short-term 2020 and long-term 2050 agendas, which set targets for increasing renewable energy (RE) production and energy efficiency for emission reductions. These undertakings bring power systems into the center of the energy transition. On the one hand it has to be able to integrate the new varying sources of decentralized energy and on the other hand, accommodate the increasing demand introduced by the increasing penetration rate of EVs.

1.1 Motivation

Due to increasing penetration rate of EVs, the local electric networks are most likely to be affected. These possible effects have been broadly investigated by recent publications. Authors of [3–5] display that even at low penetration rates EV charging could cause congestions and undervoltages in the electric network. Also the concerns over EV charging increasing the electric network losses and causing accelerated aging of the distribution transformer are addressed in [6–10]. In this new situation, the old „fit-and-forget“ approach implies that the DSOs must upgrade the existing electric networks to withstand the new, continuously increasing demand. This would mean heavy investments for the DSOs [11–13].

Therefore most of the aforementioned studies propose an alternative approach to mitigate the EV charging impacts. By charging the EV batteries in a controlled manner, the heavily congested peak load times and undervoltages can be avoided [6–10]. As the EV charger technology for Vehicle-to-Grid (V2G)[1] becomes more common, the batteries could be utilized as short term energy storage. This short term energy storage could be used by the DSO for e.g. to reduce the electric network congestion caused by the conventional loads [14]. Enabling controlled charging could also help maximize the integration of the decentralized energy generation by RE [15].

However, the controlled EV charging cannot be easily implemented as it involves multiple stakeholders each having their own interests. The first stakeholders can

[1](V2G) is a term of technology that enables the EV batteries to not only be charged but also to discharge the electricity to the electric network.

be identified as the EV owners, addressed from now on as „EV users“. EV users want to charge their EVs as fast as possible in order to have them ready for use again. The second stakeholders are identified as the charging service providers, addressed from now on as „EV fleet aggregators“. The EV fleet aggregators aim to minimize the charging costs for the EV users as well as to maximize their own profit by optimizing the electricity procurement times. However the EV fleet aggregators may have access to large EV fleets, which provides certain control potential. The third stakeholders are the DSOs whose responsibility and interest is to maintain the electric networks operational with high efficiency. Therefore, common rules are needed to enable the real implementation of controlled charging. In Germany, such a rule set is proposed by [16] as „traffic light concept“.

The report [16] specifies that „the aim of the traffic light concept is to define the sharing of functions between the regulated and the non-regulated area in terms of the control of suppliers and consumers so as to ensure permanent system stability and a free market for smart products“. The traffic light concept further specifies that, the DSOs' responsibility is to determine the current and forecast condition of their electric network areas by three traffic light phases: „green“, „amber“ and „red“.

The green phase indicates that the electric network operates under normal conditions. In green phase, the EV charging by EV fleet aggregators, are done purely on market basis. In the amber phase the DSOs are interacting with the market participants to avoid the electric network limit violations, e.g. electric network congestions or undervoltages. The red phase means that the electric network's stability is severely threatened and all the electric network operations are strictly decided by the DSOs. This information is continuously updated for the authorized market participants to handle their business accordingly and, if possible, offer services for the DSOs to reduce electric network limit violations [16]. These ideas, presented by the traffic light concept, can be taken as guidelines for developing future charging strategies for realistic implementation. Therefore this thesis focuses on developing a new charging strategy, which distinguishes the different entities and their responsibilities.

1.2 State of the Art in EV Charging Strategies

The earlier publications, regarding EV charging strategies, can be sorted into groups based on the emphases upon the aforementioned stakeholders. The first group gathers the publications emphasizing the EV fleet aggregator's interests. Publications from this group share a common objective, which is to minimize the energy procurement cost for charging EVs. In [17–20] authors propose to achieve the minimum charging costs by optimizing the EV charging power and time according to cost signal which ultimately results in globally flattened load profile. In addition to cost minimization, authors in [21–23] propose to utilize V2G to provide ancillary service for the DSO to enable congestion management.

The Second group emphasizes the DSO's interests. Also publications from this group share a common objective, which is to mitigate the EV charging impacts on the electric network. Authors in [24] aim to maximize the energy delivered to the

EVs while accounting for electric network current and voltage limits. Papers [25, 26] aim to minimize the electric network losses caused by the EV charging by optimizing the charging times and powers. Authors in [27, 28] propose EV charging control to be performed with valley filling and load shifting objectives subjected to EV battery energy constraints.

The third group, however, more clearly accounts for all of the different interests presented by the stakeholders. For this thesis the third group provides the most important insights. Therefore many of the publications from this group are briefly reviewed and subsequently the adopted ideas from these publications are presented.

Authors of [29] propose an iterative charging scheduling method which separates different stakeholders as individual entities. The charging strategy relies on continuous information exchange between the EV fleet aggregator, who is in charge of the EV charging scheduling, and the DSO, who verifies the schedules or relays constraints for the EV fleet aggregator. All stakeholder requirements are taken into consideration by passing around schedule suggestions and constraint signals between the two entities until an all constraints fulfilling solution is found. Different methods to specify electric network constraints are compared and their corresponding performance analyzed. The charging schedules and charging power rates are solved by iterative quadratic programming with cost minimization objective.

Charging strategy for three phase system is implemented in [30]. The scheduling is performed based on cost objective subjected to electric network specific constraints. The charging schedules and charging power rates are optimized by solving linear programming problems inside one entity combining all the interests. The charging strategy utilizes load flow calculations for the electric network constraints. In the strategy implementation, a moving window optimization is used to enable the on-line simulations.

Paper [31] presents a charging strategy that also separates different stakeholders as individual entities. In this charging strategy, the charging scheduling entity has complete knowledge of the electric network sensitivities and conventional loads. The EV fleet aggregator collects and forecasts the details of the EV demands and availabilities, which are submitted to the scheduling entity. The scheduling entity defines the charging schedules and power rates by linear optimization. The optimization is done based on charging cost minimization subjected to electric network and EV related constraints. After the schedules have been optimized, they are sent back to the EV fleet aggregator who executes the EV charging. Also this paper uses the moving window implementation for their charging strategy.

Study [32] investigates the impacts of strictly cost based charging on the Danish electric network and proposes an alternative approach based on power capacity availability. The authors point out that the strictly cost based charging would in fact have an adverse effect on the electric network. The alternative approach utilizes the DSO as a charging scheduling entity that could optimize the charging schedules and power rates based on costs while taking into account the substation transformer capacity limits.

Paper [28] presents a charging strategy that aims for load shifting and valley filling. They compare how different charging power rates effect their charging strategy's capability to flatten the global load profile. They demonstrate through a case

study how their charging strategy can result in completely flat load profile in the United Kingdom with a certain charging power rate and a certain EV penetration rate.

Authors of [33] propose that the Use-of-System tariffs could be implemented to influence the cost based charging. They demonstrate through a case study that the „capacity prices are an efficient instrument to account for local electric network situations in the charging schedules“. Also the EV fleet aggregators profit was guaranteed.

Based on the literature review, common ground with the earlier publications can be found. The similarities between the existing charging strategies and the most applicable ideas adopted for this thesis can be summarized as follows.

1. Most of the reviewed publications consider the charging cost minimization as primary objective and this is also adopted for this thesis. Paper [28] has an objective function that aims for peak shifting and load valley filling. This objective is adopted for one of the charging strategies used for the comparison.

2. Authors of [29–31] utilize the load flow equations for minimum voltage and maximum current constraint calculations. This is found to be an important and a reliable method to estimate the future line currents and node voltages. Thus it is also used in this thesis.

3. Papers [29, 30, 32] use realistic electric network models with statistical load profiles. Authors of [29, 31] model the EVs with dynamic behavior based on the state of battery energy. A realistic electric network model, an EV model and a few data sets are also used in this work to study the electric network impacts and performance of the new charging strategy.

4. Authors of [30, 31] implement their strategies using moving window optimization. Both studies show that the moving window optimization proves to be a reliable method even when a certain percentage of forecast errors are applied in the used data. The same implementation is also utilized in this thesis as it provides a robust method for various different objectives [30], and most importantly it enables the on-line simulations. By on-line simulations the dynamic behavior of the models can be used by the new charging strategy.

1.3 Problem Formulation

To develop a realistic charging strategy, the EV fleet aggregator and the DSO need to be separated as individual entities. Their communication needs to be arranged in a manner which does not require considerable amount of communication iterations and still enables flexibility for both entities. The EV charging needs to be arranged in a manner that all the different stakeholder requirements are addressed. Therefore, in this thesis the EV charging scheduling poses the main problem. The only control variable to solve this problem is a discrete charging time. Each of the EVs, introduced to the electric network, needs to be scheduled in a way that a cost minimization objective is achieved. In the scheduling process the following points should be accounted for:

1. Electric network power, current and voltage limits
2. Household load profiles
3. Electricity prices
4. EV availability
5. EV demand based on the realistic EV model
6. Continuous EV charging

Based on these specifications, the new charging strategy is developed in chapter 2.

1.4 Thesis Objectives

The main objective of this thesis is to develop and test a new charging strategy for realistic implementation. The second objective is to analyze the performance of the new charging strategy by comparing it against a Uncontrolled Charging Scenario (UCS) and three existing charging strategies, which are derived from the earlier publications. In addition, the third objective is to investigate and compare the effects of two EV fleet aggregators, which are equipped with two different charging strategies, on the electric network.

In this thesis the DSO and the EV fleet aggregator are separated and their communication is carried out by technical signals issued by the DSO. In a single EV fleet aggregator simulations, this communication does not require iteration. These technical signals distinguish feeder wise and global wise power capacities available after the household loads have been accounted for.

1.5 Thesis Scope

This thesis mainly concentrates on developing and testing a new charging strategy. The proposed charging strategy is described and compared against existing charging strategies. The performance is assessed in terms of aforementioned stakeholder interests. The focus is on EV charging scheduling, which is done by different charging strategies. All of the charging strategies are assuming perfect forecasts for the used data. In this work the EVs are considered to be charged at home with the rated power of the charger. Both, the V2G capability and the EV battery's aging are not investigated. Also the influence of increased EV charging during night time on the global electricity price development is not investigated.

1.6 Justification

When considering the guidelines received by the traffic light concept and the realistic implementation of the controlled charging, some shortcomings can be found from the earlier publications reviewed in section 1.2. Based on the proposal in [31], the scheduling entity has clearly the role of the DSO as it has the complete knowledge of the electric network line currents, node voltages as well as the forecasts for the conventional loads. The EV fleet aggregator's role is merely to provide the EV energy

demand forecasts and to execute the plans received from the scheduling entity. In a similar manner, authors of [32] propose that the DSO acts as a scheduling entity who collates the information regarding the EV availability and the demand from individual EV users. After the scheduling process, the DSO submits the schedules for the individual EVs.

From the charging decision making point of view these aforementioned approaches are similar to [30] whose charging strategy clearly combines the EV fleet aggregator and the DSO into one. Paper [29] on the other hand emphasizes a more acute division in the roles as it uses the DSO to verify the schedules made by the EV fleet aggregator. In case electric network congestion or undervoltages occur, the schedules are solved iteratively which in reality might take a long time. The decision making duration was not discussed as this charging strategy was not developed for on-line simulations. In this thesis the DSO and EV fleet aggregator are considered as completely individual entities with their own responsibilities and limited communication to save time in the charging scheduling.

Moreover, the approach differences between the earlier publications and this thesis are apparent. Study [33] presents a market based approach for the DSO to interact with the EV fleet aggregator. However, in this thesis the interaction is to be handled by a technical signal. In this fashion, authors of [32] propose that the global power capacity for EV charging is calculated by the DSO based on the EV availability and the demand. However, this thesis distinguishes feeder wise and global wise power capacities, which are calculated after the household loads have been accounted for.

Also the differences in the charging strategy implementations are clear. Authors of [29–31] implement only one charging strategy while [32] implements two charging strategies and compare their impacts on the electric network. None of the reviewed publications implement and compare four different charging strategies along with the UCS.

Furthermore, none of the reviewed publications investigate and compare the effects of two EV fleet aggregator, equipped with two different charging strategies, on the electric network.

1.7 Outline of the Thesis

The new charging strategy and the existing charging strategies are developed and formulated as optimization problems in chapter 2. It also develops the implementation for multiple EV fleet aggregators and introduces the optimization environment. The developed charging strategies are implemented into a simulation system, which is introduced in chapter 3. In the same chapter, the used simulation models and the used data are presented. The case studies for the simulations are presented and results analyzed in chapter 4. Finally chapter 5 summarizes the work carried out as part of this thesis and presents the conclusions of the new charging strategy. Lastly, it gives proposals for future research.

Chapter 2

Charging Scheduling Strategies

In this chapter, the existing strategies and the new charging strategy are developed. In all of the charging strategies, the EV fleet's charging is scheduled by optimizing the binary matrix $\mathbf{x}$ [1], as introduced in section 1.3. The EV users prefer charging without interruption and this is realized in the UCS. To respect the EV users preferences for the continuous charging, all of the strategies are equipped with dual objective functions. The secondary objective specifies that the charging should be done continuously once it has started.

However, the primary objectives and the rest of the input information vary depending on the strategy. These different strategies are introduced in their individual sections where their related mathematical optimization problems are also formulated. Subsequently the optimization environment is presented and the moving window implementation is introduced. All of the flowcharts, introduced for each of the strategies, contain connection point indicators namely Start CS and End CS. These are used to indicate each of the individually presented strategies as a small part of the main algorithm introduced in section 3.5. In all of the flowcharts the scheduling decision making entities are always surrounded surrounded with green dashed lines. The „EV fleet charging schedules“ are referred from now on as „EV schedules“.

2.1 Uncontrolled Charging Scenario (UCS)

The UCS describes the uncontrolled charging behavior of the EV users. All of the EV users are expected to charge their EVs right away after their day's activities so that the EVs are with enough charge for the next day or for the next trip. The UCS is expected to be the most expensive and it might also cause the largest charging impacts on the electric network out of all charging strategies. These outcomes for the UCS can be assumed based on the statistical mobility data and the used household load profiles, presented in chapter 3.

2.2 Aggregator Based Strategy (ABS)

The ABS can be derived from the first group, presented in section 1.2, which gathers the publication emphasizing the EV fleet aggregator's interests. Figure 1 illustrates the inputs and outputs for the ABS, which is the scheduling decision making entity. Here the ABS optimizes the EV schedules with charging costs minimization as primary objective, regardless of the electric network constraints.

[1] Throughout the thesis the boldfaced characters are used for vectors and matrices. In addition the black-boarded characters specifies that they are in complex form, e.g. $\mathbb{V}$ for complex voltage, and the italic characters signify that they are real scalars.

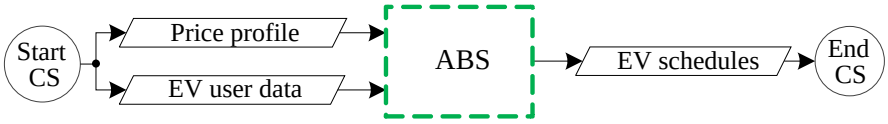

Figure 1: Inputs and outputs for the ABS

Therefore the ABS is expected to attain the lowest charging costs out of all charging strategies. On the one hand, the ABS might work with a low EV penetration rate in case the prices are low during night time when the household loads are also low. On the other hand, the price profiles, as introduced in chapter 3, might have low cost electricity during the other wise congested time. This could lead the ABS causing further congestion in the electric network even with a low EV penetration rate.

To use this strategy, the aforementioned objectives are formulated as dual objective function presented as follows:

$$\begin{aligned} \underset{=\tau}{\hat{\mathbf{x}}} &= \arg \min_{\mathbf{x}\in\{0,1\}^{(n,\tau)}} f(\mathbf{x}) \quad \text{s.t.} \quad \boldsymbol{\Upsilon} \\ f(\mathbf{x}) &= \sum_{n\in N}\sum_{\tau\in T} \left(\mathbf{C}_\tau \cdot P_{\mathrm{EV}} \cdot \mathbf{x}_{n,\tau} \cdot \Delta\tau + C_{\mathrm{P}} \cdot |\mathbf{x}_{n,\tau} - \mathbf{x}_{n,\tau-1}|\right), \end{aligned} \tag{2.2.1}$$

where

- $\boldsymbol{\Upsilon}$ is a vector of EV user constraints;
- T is the set of time steps within an optimization window;
- N is the set of nodes with an EV connected;
- $\mathbf{C}_\tau$ is the electricity price at time step τ;
- P_{EV} is the rated charging power for all the EVs;
- $\mathbf{x}_{n,\tau}$ is the charging schedule of the nth EV at time step τ (1 for charging, 0 for not charging);
- $\Delta\tau$ is the length of a time step.
- C_{P} is the constant cost penalty factor for the secondary objective;

The function of the C_{P} is merely to encourage the optimizer (solver) to arrange the charging in a continuous manner. The C_{P} is not taken into consideration in the final cost calculation for the EV fleet charging. To specify the constraints, the EV energy demand $\mathbf{E}_{\mathrm{EV},n}$ of the nth EV is calculated from the EV user data by:

$$\mathbf{E}_{\mathrm{EV},n} = \gamma_{\mathrm{batt}} \cdot (SoC_{\mathrm{full}} - \mathbf{SoC}_{\mathrm{EV},n}), \tag{2.2.2}$$

where the γ_{batt} is the battery capacity, SoC_{full} is the state of charge for full battery and $\mathbf{SoC}_{\mathrm{EV},n}$ is the battery state of charge of the nth EV. The EV demand is used to formulate the first constraint in (2.2.3), which specifies that by the end

of the scheduling window, introduced in section 2.7, all of the EVs should be fully charged.

$$\Upsilon_1 : \qquad \sum_{\tau \in T} \left(P_{\mathrm{EV}} \cdot \mathbf{x}_{n,\tau} \cdot \Delta\tau \right) = \mathbf{E}_{\mathrm{EV},n}, \;\; n \in N. \tag{2.2.3}$$

The EV user data is also used to derive the second constraint which is the EV availability for the charging. It is considered as an equality constraint and can be presented by:

$$\Upsilon_2 : \mathbf{x}_{n,\tau} = \begin{cases} 1 & \text{for EV is available for charging} \\ 0 & \text{for EV is not available for charging} \end{cases}, \;\; n \in N, \;\; \tau \in T. \tag{2.2.4}$$

The charging scheduling for a individual EV is only possible if the binary value for a specific time slot is logical „true“ (1), meaning that the EV is available for charging. The charging scheduling is not possible if the corresponding time slot is logical „false“ (0), meaning that the EV is not available for charging. The constraints (2.2.3) and (2.2.4) being collected symbolically in the vector $\boldsymbol{\Upsilon} = [\Upsilon_1, \Upsilon_2]$ are also used by all the other strategies and are referred there by the vector symbol $\boldsymbol{\Upsilon}$.

2.3 DSO Based Strategy (DBS)

The second group, presented in section 1.2, is used to formulate the DBS as it gathers the publication emphasizing the DSO's interests. The DBS is expected to be by far the most electric network friendly strategy as its main objective is to shift the load peaks and fill the load valleys. The inputs and outputs for the DBS, which is here the scheduling decision making entity, are illustrated in Figure 2.

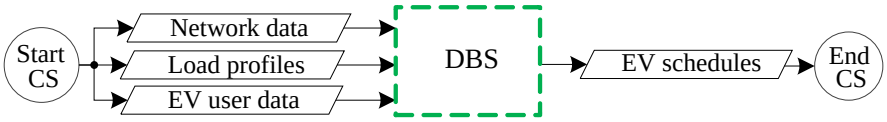

Figure 2: Inputs and outputs for the DBS

However, this strategy can be expected to be more expensive than the other three strategies. Despite that fact, the DBS can offer a reference point for network losses, as they are expected to be the smallest in this strategy. Paper [25] proves that the load profile flattening has positive influence on network losses. Network losses could be even reduced by the EV charging up to a certain extend. The primary objective is taken from publication [28], and the whole objective function is formulated as follows:

$$\begin{aligned} \underset{=\tau}{\hat{\mathbf{x}}} &= \arg \min_{\mathbf{x} \in \{0,1\}^{(n,\tau)}} f(\mathbf{x}) \quad \text{s.t.} \;\; \boldsymbol{\Theta}, \boldsymbol{\Upsilon} \\ f(\mathbf{x}) &= \sum_{\tau \in T} \sum_{n \in N} \sum_{h \in H} \left[\left(P_{\mathrm{EV}} \cdot \mathbf{x}_{n,\tau} + \mathbf{P}_{\mathrm{hh},h,\tau} \right)^2 + P_{\mathrm{P}} \cdot \left| \mathbf{x}_{n,\tau} - \mathbf{x}_{n,\tau-1} \right| \right], \end{aligned} \tag{2.3.1}$$

where

- $\mathbf{\Theta}$ is a vector of electric network constraints;
- H is the set of nodes with a household connected;
- $\mathbf{P}_{\mathrm{hh},h,\tau}$ is the power demand of the hth household at time step τ;
- P_{P} is the constant power penalty factor for the secondary objective.

Also here the P_{P} is a factor addressed only for the solver. The network data and the load profiles, presented in Figure 2, provide all the needed information for the technical constraints. The technical constraints considered are the maximum total load which is taken from the load profile as the maximum annual load P_{max}, the maximum currents $\mathbf{I}_{max}$ and the minimum and maximum voltages V_{min} and V_{max}. They are applied as inequality constraints for each time step. The Equation (2.3.2) defines that the summation of the total EV charging power and the total demand of the household loads have to be equal to or lower than the admissible power limit.

$$\Theta_1 : \qquad \sum_{n\in N} \left(P_{\mathrm{EV}} \cdot \mathbf{x}_{n,\tau}\cdot\right) + \sum_{h\in H} \left(\mathbf{P}_{\mathrm{hh},h,\tau}\right) \leq P_{max}, \;\; \tau \in T. \tag{2.3.2}$$

The voltage and current constraints are formulated with the help of appendix A. For the constraints, the voltage $\mathbb{V}_{\mathrm{ref},m}$ of the mth node and current $\mathbb{I}_{\mathrm{ref},l}$ of the lth line are calculated according to the given recommendations. They describe a constant reference point for the voltage and current estimation. The voltage constraint can be expressed as:

$$\Theta_2 : \qquad \begin{array}{l} V_{min} \leq |\mathbb{V}_{\mathrm{ref},m} + \Delta\mathbb{V}_{\mathrm{hh},h,\tau} + \Delta\mathbb{V}_{\mathrm{EV},n,n} \cdot P_{\mathrm{EV}} \cdot \mathbf{x}_{n,\tau}| \leq V_{max} \\ m \in M, \;\; h \in H, \;\; \tau \in T, \;\; n \in N \end{array}. \tag{2.3.3}$$

The Equation (2.3.3) describes that all of the electric network voltages need to be equal to or higher than the permissible V_{min} and respectively equal to or lower than V_{max}. Here, M is the set of all nodes in the electric network. The $\Delta\mathbb{V}_{\mathrm{hh},h,\tau}$ stands for voltage change by the hth household load at time step τ for every node voltage in the electric network. The $\Delta\mathbb{V}_{\mathrm{EV},n,n}$ stands for the voltage sensitivity matrix, which defines the voltage change by the nth EV charging for every node voltage in the electric network. The last of the technical constraints prevents the overloading of any of the electric network lines, and it can be formulated as:

$$\Theta_3 : \qquad \begin{array}{l} |\mathbb{I}_{\mathrm{ref},l} + \Delta\mathbb{I}_{\mathrm{hh},h,\tau} + \Delta\mathbb{I}_{\mathrm{EV},n,n} \cdot P_{\mathrm{EV}} \cdot \mathbf{x}_{n,\tau}| \leq \mathbf{I}_{max} \\ l \in L, \;\; h \in H, \;\; \tau \in T, \;\; n \in N \end{array}. \tag{2.3.4}$$

Here L is the set of nodes where a line is ending. The $\Delta\mathbb{I}_{\mathrm{hh},h,\tau}$ stands for the current change by the hth household load at time step τ for every line current in the electric network. $\Delta\mathbb{I}_{\mathrm{EV},n,n}$ stands for the current sensitivity matrix, which defines the current change by the nth EV charging for every line current in the electric network. The constraints (2.3.2), (2.3.3) and (2.3.4) are combined symbolically in the vector $\mathbf{\Theta} = [\Theta_1,\Theta_2,\Theta_3]$.

2.4 System Based Strategy (SBS)

The publications accounting for all the stakeholder interests are described to belong in the third group in section 1.2. They are used to determine the SBS, which combines the ABS and DBS into one. This is illustrated in Figure 3 by delivering all the inputs to the SBS, which is here the scheduling decision making entity.

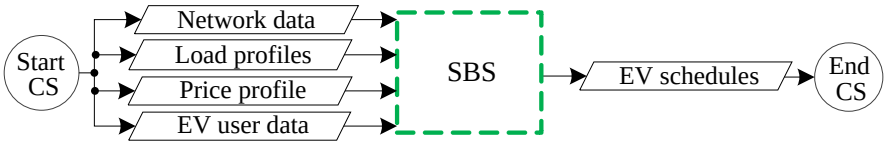

Figure 3: Inputs and outputs for the SBS

The SBS presents a compromise as it aims to minimize the charging costs while satisfying the DSO's requirements. On the one hand the SBS is expected to produce worse results when compared with the ABS and DBS on their respective main objectives. On the other hand it is the only one of the three strategies that can produce results which satisfy all the stakeholder requirements. The SBS is the most realistic of the three strategies and is therefore the main comparison point for the new charging strategy. The SBS uses the objective function (2.2.1) from the ABS and the constraints $\boldsymbol{\Upsilon}$ and $\boldsymbol{\Theta}$ similar to the DBS.

2.5 Communication Based Strategy (CBS)

The new charging strategy relies on completely individual entities and on their limited communication as pointed out in section 1.4. Therefore it is referred to as the Communication Based Strategy (CBS). It is expected to behave in a similar manner as the SBS as it still aims to satisfy all the same stakeholder interest. Even though the input information is the same, the EV scheduling process differs from the SBS. The difference is illustrated in Figure 4 where the DSO is surrounded with red dashed lines, while the EV fleet aggregator is the scheduling decision making entity.

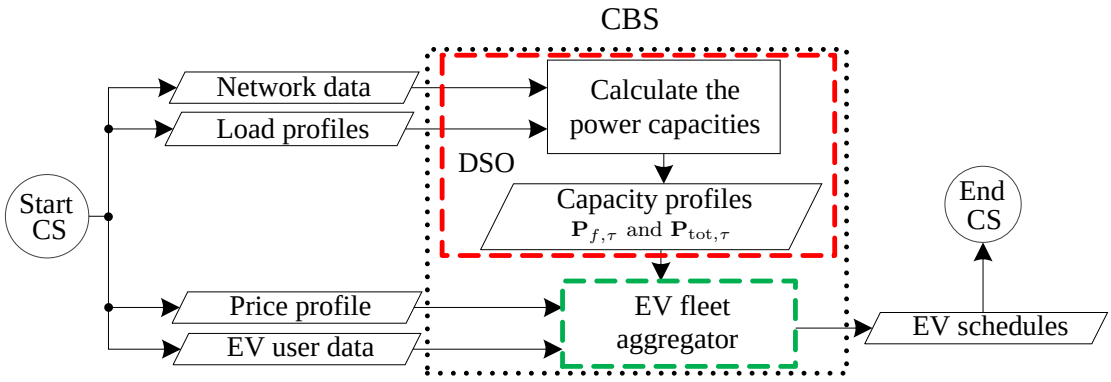

Figure 4: Inputs and outputs for the CBS

Here the technical signals issued by the DSO contain power capacity profiles for the fth individual feeder by $\mathbf{P}_{f,\tau}$ and a global power capacity profile $\mathbf{P}_{\text{tot},\tau}$ for a certain time horizon specifying each time step τ. These power capacities are calculated based on the household load forecast. This arrangement separates the DSO and EV fleet aggregator actions in a manner that the DSO will not be burdened by the detailed information regarding the EVs. Moreover, this method of communication does not require any iteration between the DSO and the EV fleet aggregator.

The EV fleet aggregator, who is the scheduling entity, is not expected to have any information concerning the electric network other than the EV locations in the electric network. The knowledge for the EV locations in the electric network and the power capacities are needed to avoid electric network limit violations. Otherwise the charging decisions are optimized based on cost minimization.

The CBS has a slightly easier optimization problem than the SBS. The SBS has to verify that the EV schedules are not causing voltage and current limit violations in any of the electric network nodes and lines. The CBS on the other hand, manages by taking care that the feeder and global power capacities are not exceeded. Thus the CBS might result in a better solution on charging cost minimization.

However, should the DSO calculations for the power capacities be proven wrong, it could lead to electric network limit violations. This could happen due to two reasons. Firstly, due to inaccurate sampling used to generate the household load profiles for the optimization process, described in chapter 4. Secondly, due to inaccuracy in the line current and the node voltage estimation, presented in appendix A. Underestimated household loads lead to too high power capacities for the EV fleet aggregator. In case electric network limit violations occur, the sampling method should be changed or the current and voltage estimation safety margin should be increased.

2.5.1 DSO's Power Capacity Calculations

To calculate the power capacities, the same technical limits are taken into consideration as with the DBS. Accordingly, the maximum available power capacities without violating the limits are calculated based on feeder currents and node voltages. The voltage and current based calculations result in different power capacities. Thus they are compared and the smaller value for each time step is used to formulate the final power capacity profile $\mathbf{P}_{f,\tau}$. The global power capacity $\mathbf{P}_{\text{tot},\tau}$ is calculated in an easier manner and it can be presented as follows:

$$\mathbf{P}_{\text{tot},\tau} = P_{max} - \sum_{h \in H} \left(\mathbf{P}_{\text{hh},h,\tau} \right), \quad \tau \in T. \tag{2.5.1}$$

These power capacities are considered as constraints by the EV fleet aggregator.

2.5.2 Scheduling by the EV Fleet Aggregator

The CBS attains the cost minimization objective function (2.2.1) as well as the vector of constraints $\boldsymbol{\Upsilon}$ from the ABS. However, the objective function is subjected to two new constraints (2.5.2) and (2.5.3), which are gathered symbolically in the

vector $\mathbf{\Gamma} = [\Gamma_1, \Gamma_2]$. The first new constraint prevents the overloading of any of the electric network's main feeders and it is formulated as:

$$\Gamma_1 : \qquad \sum_{n \in N_f} (P_{\mathrm{EV}} \cdot \mathbf{x}_{n,\tau}) \leq \mathbf{P}_{f,\tau}, \quad f \in F, \quad \tau \in T, \qquad (2.5.2)$$

The F is the set of main feeders in the electric network. The last new constraint specifies that the total charging power of all EVs should be less than or equal to the $\mathbf{P}_{\mathrm{tot},\tau}$ and it is formulated as:

$$\Gamma_2 : \qquad \sum_{n \in N} (P_{\mathrm{EV}} \cdot \mathbf{x}_{n,\tau}) \leq \mathbf{P}_{\mathrm{tot},\tau}, \quad \tau \in T. \qquad (2.5.3)$$

2.5.3 Multi EV Fleet Aggregator Scenario

To develop the multi EV fleet aggregator scenario the role of electricity retailer is taken as a guideline. Electricity retailers operate in the electric network without specific network territories. This means that neighboring households may purchase their electricity from different electricity retailers. The same idea is adapted for the multi EV fleet aggregator scenario, meaning that EVs and their household locations are randomly divided among the EV fleet aggregators. Figure 5 illustrates the interaction between the two EV fleet aggregators and the DSO with a simple flowchart. A more detailed flowchart is provided in appendix B.

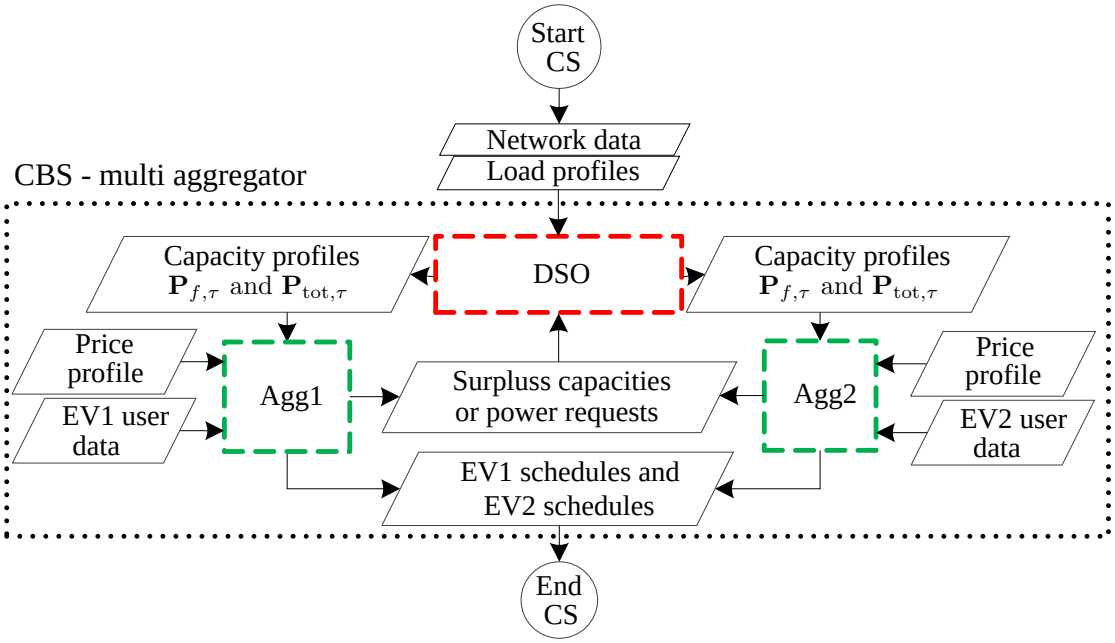

Figure 5: Flowchart of two EV fleet aggregators and DSO interaction

Moreover, to implement multiple EV fleet aggregators properly, the DSO divides the power capacities among the EV fleet aggregators according to their size. Reduced power capacity might lead to a situation where the received power capacity

is insufficient for charging. Therefore the communication between the DSO and the EV fleet aggregator is relaxed to enable two way communication. However the communication is facilitated in a manner that requires only one additional iteration compared to the single EV fleet aggregator scenario.

The EV fleet aggregators try to optimize the EV schedules according to their individual inputs. If the EV fleet aggregator fails in the charging scheduling due to insufficient power capacity, it will issue a power request. The DSO may provide extra power capacity only in case the second EV fleet aggregator has succeed in the charging scheduling and submitted the surplus capacities to the DSO. In case both EV fleet aggregators fail, the DSO can only re-send the old power capacities to the EV fleet aggregators. After receiving the second power capacity profiles, the EV fleet aggregator performs the charging scheduling optimization again. In the event of a new failure, the final SoC target is reduced to the extent that the EV schedules can be optimized.

2.6 Optimization Tool

In this thesis the CVX toolbox, a package for specifying and solving convex programming problems [34], [35], is used to solve the different optimization problems. The DBS is programmed as a constraint binary quadratic programming problem whereas all of the other strategies are programmed as constrained binary linear programming problems. To solve these problems, two different solvers, Mosek [36] and Gurobi [37], are used because of their capability to solve binary problems. Their usage is illustrated in Figure 6.

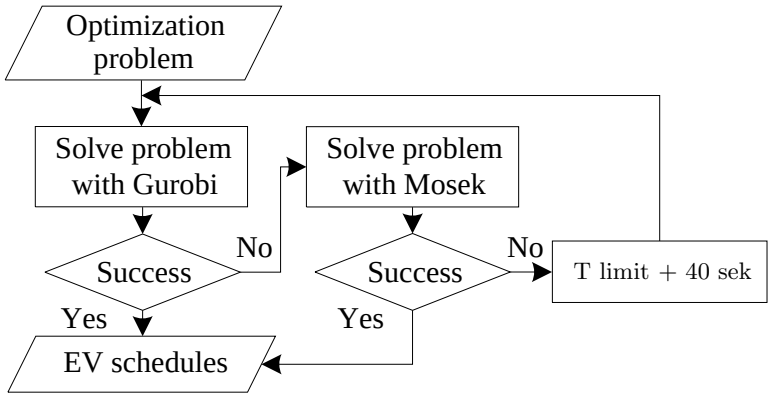

Figure 6: Flow chart for the solver usage

This arrangement is needed because in linear optimization problems Gurobi is faster than Mosek, however in quadratic optimization problems Mosek is faster. The used binary variables complicates the optimization problems, therefore the time limitation is added to guarantee that time spent in solving the problem is kept within reason. The quadratic optimization problems are more exhaustive for the solvers and that is why the additional time may be required.

2.7 Moving Window Optimization

As mentioned in section 1.2, the strategies are implemented using moving window optimization to enable the on-line simulations and to attain the dynamic behavior of the simulation models. In the moving window optimization, the used strategy requires forecast data for a fixed time horizon. The temporal behavior of a moving window optimization is presented in Figure 7.

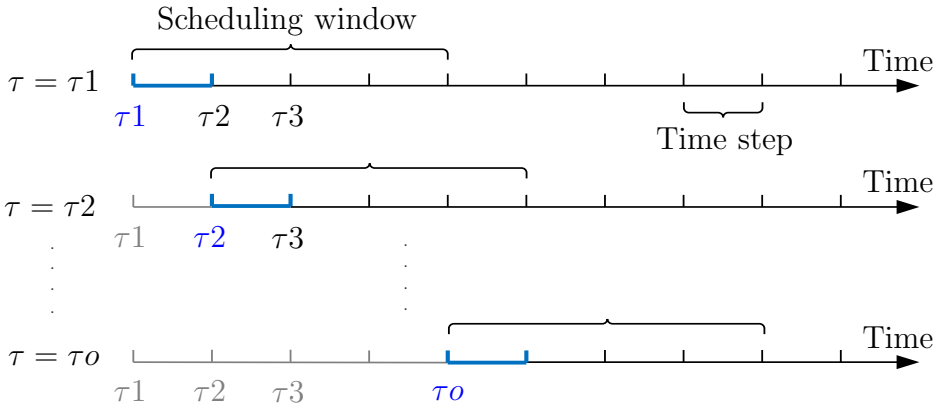

Figure 7: Illustration of the moving window optimization

Based on the available information, the used strategy optimizes the EV schedules for the current scheduling window. Even though the optimizer results in EV schedules for several time-steps, only the decisions for the current step, which in Figure 7 is indicated in blue, is utilized. According to the EV schedules for the given time-step, the EVs are charged in the simulation model and the received output parameters are stored. As time progresses the scheduling process is repeated with updated forecast data, and the latest simulation parameters. This results in new EV schedules for the current time step. This enables flexibility on random EV arrivals and mitigates the impacts of forecasting errors [38]. In all of the strategies, the EV related information is received at the instant it becomes available for charging.

Chapter 3

System Modeling

To test the developed charging strategy and study its effects on the electric network, a simulation system model containing the realistic models for the electric network and the EV are developed. A simplified illustration of the whole simulation system is presented in Figure 8.

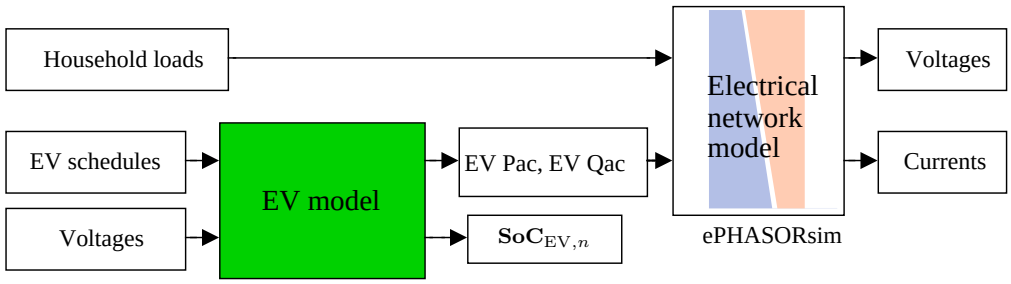

Figure 8: Simulink model for the simulation system

These models are developed in the MATLAB/Simulink [39] environment with additional toolbox provided by Opal-RT. This provides the ePHASORsim solver, which enables the dynamic simulations of large scale power systems in Phasor mode [40]. ePHASORsim can simulate thousands of nodes, generators, transformers, transmission lines, loads and controllers. This tool enables the on-line mode tests for the developed charging strategy. In this chapter the electric network model is described. Subsequently the vectorized EV charging model, the applied data sources and the work flow of the main algorithm are presented.

3.1 Electric Network Model

The used electric network model represents a typical suburban area in Germany. It is the largest Low Voltage (LV) network generated in [41]. The details for this synthetic electric network model are taken from the dissertation [42]. The topology of the chosen electric network is presented in Figure 9.

This LV-network is equipped with a 630 kVA distribution transformer and it has 10 main feeders whose cables have a maximum current limit $I_{max} = 284\ A$. The used LV-network consist of 294 nodes where 146 households are located. These households are randomly selected to accommodate an EV. The applied EV penetration rates are 75%, which means that 110 of the households are accommodating an EV, and 100% which means that all of the households are accommodating an EV.

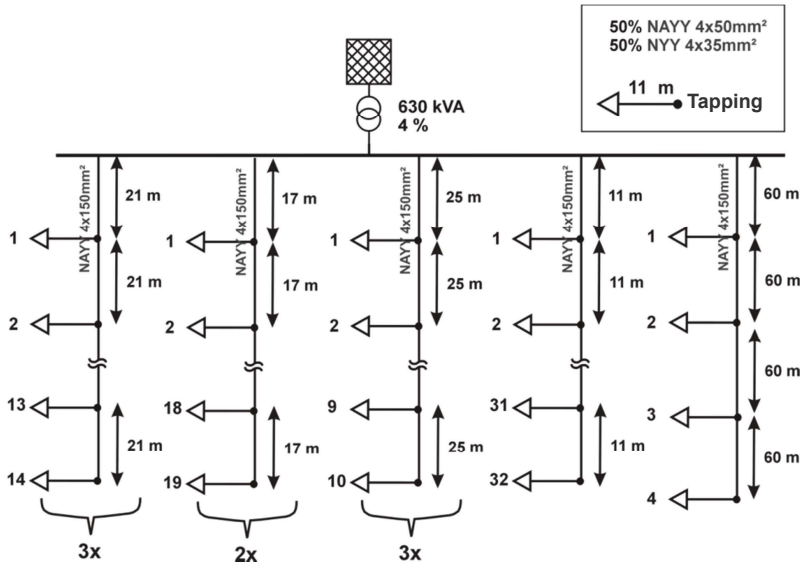

Figure 9: Topology of the used electric network [42].

3.2 EV Charging Model

The EVs can be modeled as systems composed of many dynamic dependencies. The key components in the EV models are the charger and the battery. The EV model used in this thesis is sourced from [10]. It consists of blocks for the driving schedules, charger logic, converter losses and the battery model as presented in Figure 10. The driving schedule block collects and passes on the data regarding the EV ID, EV address and the EV demand $\mathbf{DoD}_{\mathrm{EV},n}$. The EV demand describes the Depth of Discharge (DoD) of the nth EV. The EV ID specifies which of the EVs are connected and the address specifies the household node for each EV. As soon as an EV is connected to the electric network, the driving schedule block relays the details for the charger logic block and updates the battery DoD information to the battery model block.

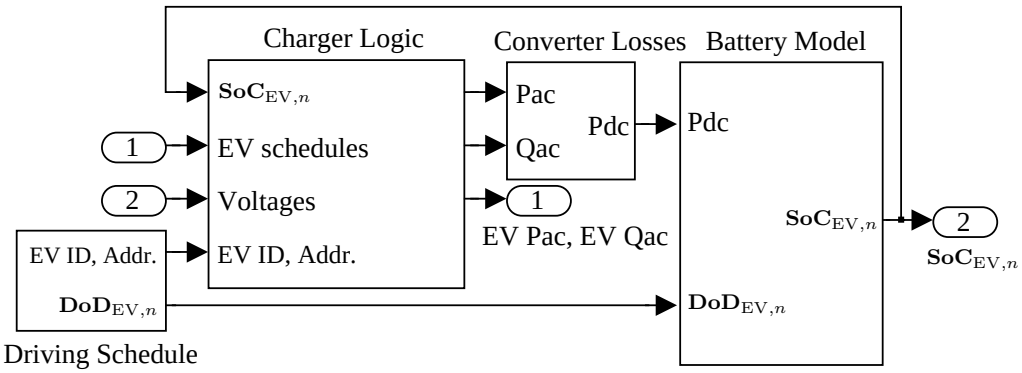

Figure 10: Simulink model for the EV

The charger logic block receives data from four sources. The first input comes from the battery model block, which continuously updates the charger logic block

with the current $\mathbf{SoC}_{\mathrm{EV},n}$. The second input comes from the EV fleet aggregator who submits the EV schedules. These schedules are directly used by the charger logic block. The third input receives the current voltages from the electric network model. The fourth input comes from the driving schedule block, and contains the information explained earlier.

The charger's main function is to convert the AC power into DC power, which is required to charge the battery. The charger logic block processes the received data and regulates the battery charging in a manner that the local network voltage limits, set for each EV separately, are not violated. It also computes the appropriate charging power rates as they are dependent on the batteries' $\mathbf{SoC}_{\mathrm{EV},n}$ levels as explained by [10]. This phenomenon is explained in appendix C and is visualized in Figure 32. The charger losses are calculated in the Converter losses block. The remaining DC power is delivered to the battery model block until the $\mathbf{SoC}_{\mathrm{EV},n} = SoC_{\mathrm{full}} = 0.9$ is reached.

This EV model is tuned to present the charging behavior of Mitsubishi iMiEV as part of this thesis. It is equipped with $\gamma_{\mathrm{batt}} = 16,5\ kWh$ battery and the applied charging power is $P_{\mathrm{EV}} = 3,7\ kW$. The EV validation work is presented in appendix C. Moreover, the capacitive characteristics and the temperature characteristics of the battery are not considered in this model.

3.3 Driving Behavior of the EV Users

In this thesis, the surveyed dataset collected by the project „Mobility in Germany 2008“ [43] is used to generate the EV user behaviors. The mobility survey covers information for different weekdays, ways of transportation, journey lengths and journey start & end point destinations. It was collected by interviewing people from thousands of households in the year 2008. This data is sorted out to fulfill the below mentioned requirements:

- Only passenger cars are considered
- Only home arriving journeys are considered
- Single journey length is less than 100 km

The wanted amount of EV user behaviors are randomly selected from the database for each EV penetration rate respectively. The used data is assumed to be season independent. As the EV model is chosen as Mitsubishi iMiEV, it is possible to calculate the correct energy consumptions for each trip. The manufacturer [44] informs that energy consumption for this model is $E_{km} = 0,1\ kWh/km$. Accordingly the function for energy demand can be formulated as follows:

$$\mathbf{DoD}_{\mathrm{EV},n} = \frac{\gamma_{\mathrm{batt}}}{\sigma_{\mathrm{EV},n} * E_{km}}, \tag{3.3.1}$$

where $\mathbf{DoD}_{\mathrm{EV},n}$ is calculated according to $\sigma_{\mathrm{EV},n}$ which describes the distance driven by nth EV.

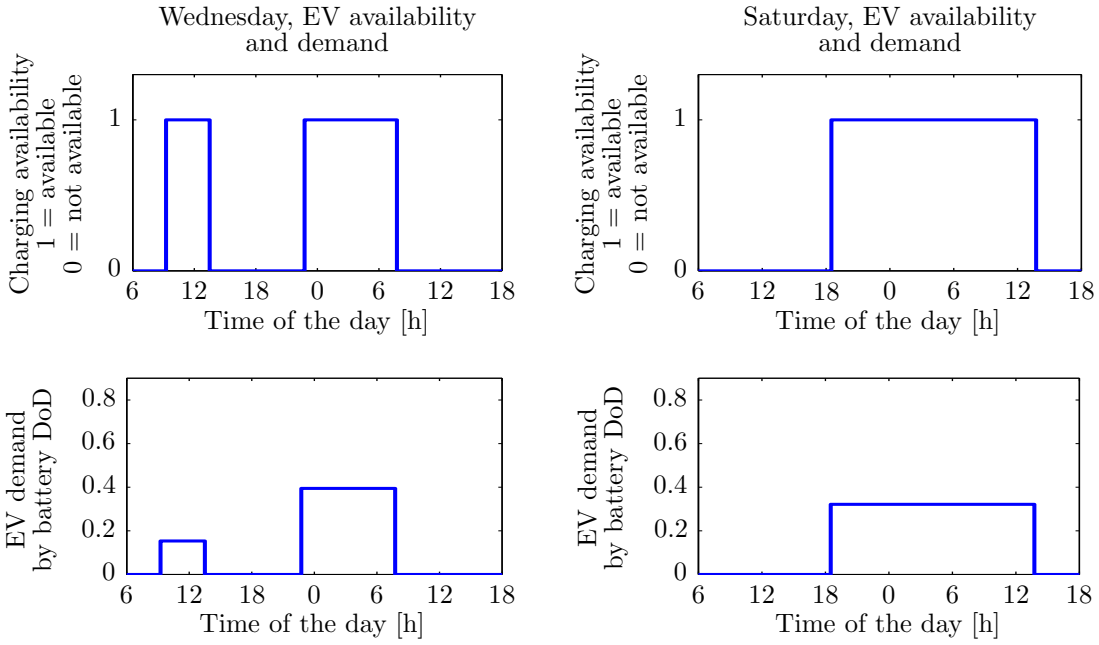

Figure 11: EV availability and demand on a Wednesday and a Saturday

Figure 11 represents the behavior of one EV on a Wednesday and a Saturday. On a Wednesday it is available for charging on two time periods and for one time period on Saturday. Correspondingly it has a different battery DoD for each availability periods respectively. As explained earlier, the data describes all the journeys happening during the day. In case multiple journeys occur, the availability periods, which are less than two hours, are neglected for every simulation and for every charging strategy to be consistent.

3.4 Household Load and Electricity Price Profiles

Each electric network has a certain type of demand (load) profile and is greatly influenced by the type of customers. For simplification, only residential customers are considered in this thesis. The dataset used in this work contains synthetically generated load profiles of German households based on statistics. The dataset is taken from the work [45]. The household load profiles for 146 households are picked stochastically from the given dataset.

It is assumed that each household has a constant power factor of 0.9, which is used to calculate the apparent power in the electric network. The used data has a resolution of 1 minute, which defines the time resolution used in the simulations. Figure 12 presents the cumulative household load profiles and the electricity price profiles for the chosen days. The charging strategies are tested with a data for Wednesday-Thursday and Saturday-Sunday time periods. Based on random selection the data is taken from the 16th week of the year 2013. Figure 12 describes the used data covering a time period of 48 hours from the first day 00:00 o'clock till the second day 23:59 o'clock. It is ensured that the EV availability time is covered as the EV availability in most of the cases occurs over night, as illustrated in Figure 11.

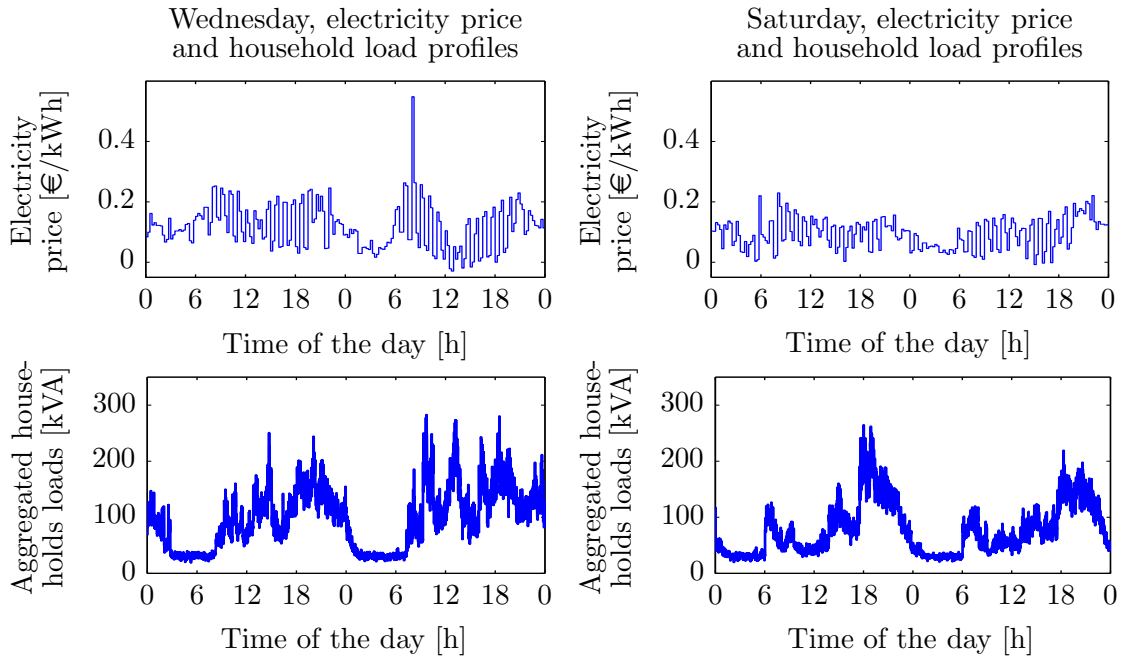

Figure 12: Aggregated household load and electricity price profiles on a Wednesday and a Saturday

As the key objective of the developed charging strategy is to minimize the charging costs of the EV fleet, a proper price profile is needed. The price profiles are taken from the European Power Exchange (EPEX) spot market database [46] which offer historical data for intra-day price profiles in 15 minute resolution. The intra-day price profiles are used because a perfect forecast is assumed. The received price profiles are multiplied by 4 to account for the taxes and fees [47]. The resolution of the given price profile defines the time step, introduced in section 2.7, which is used in the optimization. According to the above description, one simulation step is 15 minutes long and it is performed in 1 minute resolution.

3.5 Work Flow of the Main Algorithm

The test algorithm consisting both, charging strategies and system model, are presented by a flow chart in Figure 13. This specifies the different process phases and specifies at which phase the charging strategies are used. The simulation system in Simulink and the main algorithm in MATLAB uses a shared memory for the individual processes. First the system is initialized where all the needed inputs are prepared. As part of the initialization the simulation model is executed in order to obtain the initial EV energy demands $\mathbf{E}_{\mathrm{EV},n}$ for the optimization. Subsequently the needed profiles are selected for the current simulation step and for the optimization window. Then the EV information is investigated and in case none are available, the charging scheduling phase is bypassed and the current time step is directly simulated. The same is repeated for every simulation step, based on the latest simulation parameters and information about the EVs.

In case at least one EV is available and in need of charging, the charging scheduling algorithm is executed. The chosen charging strategy selects the needed input

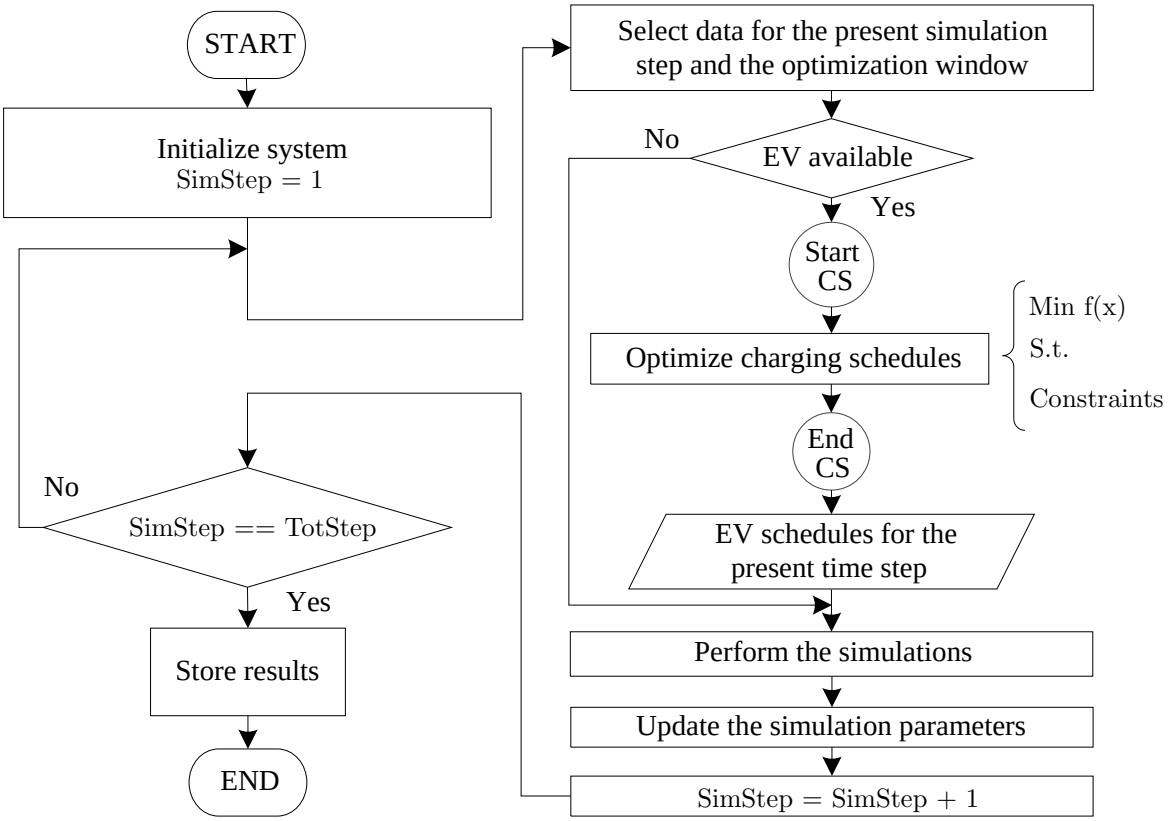

Figure 13: Flow chart of the simulation process

profiles as presented in chapter 2. After the scheduling process, the EV schedules are updated for the current time step and used in the simulations as explained in section 2.7. The main algorithm iterates until the end of the wanted time, which is indicated by „TotStep“ in Figure 13.

Chapter 4

Case Studies and Evaluation

In this part the simulation results by different case studies are presented and evaluated. The aspects related to EV user's comfort are analyzed in terms of the EV fleet total charging cost, change of charging cost, net number of interruptions and the time flexibility. The total charging costs are calculated for every strategy according to the given electricity price profiles. The change of the charging costs are calculated for both of the case studies in comparison to the results received by using the UCS for the whole EV fleet. The change of the charging cost is measured in percentages.

Moreover, the charging is expected to be done without charging interruptions, as explained in chapter 2. To evaluate how different strategies perform, the net number of interruptions, occurring in the whole EV fleet charging, is calculated. For this, the UCS is also used as reference point. In some cases the net number of interruptions is negative. This indicates that the corresponding charging strategy manages to charge some of the EVs, which have multiple journeys during the day, in one charging session. It also means that these EVs have enough electricity in the battery to perform the second journey and to be completely charged in a single charging session. Furthermore, the time flexibility indicates the average amount of time the EVs have after the charging is finished and before the following day's first journey. Even though the time flexibility was not addressed by any of the strategies, it can be considered to increase the EV users' comfort as they may start the following journey earlier if needed. The time flexibility by the UCS is the longest, as the EVs are charged immediately when they are availably for charging. Therefore the time flexibility by the UCS is not considered in the evaluation.

Moreover, the results for the electric network impacts are analyzed in terms of current limit violations, network loss change and cost of the network losses. The current limit violations are measured from the first line of the most heavily loaded feeder. The current limit violations are displayed by violation magnitude, measured in percentages, and duration, measured in minutes. The change of network losses are measured in percentages. In the network loss calculations the network losses, caused by the Base load Scenario (BS), are subtracted from the results to attain and compare only the network losses caused by the EV charging with different charging strategies. After the base load subtraction, the network loss change percentages are calculated in comparison to the UCS. Moreover, the different charging strategies are considered to be accountable for the network losses they are causing. Therefore the network loss costs are calculated according to the corresponding electricity prices.

None of the performed simulations violated the voltage limits, which are $\pm 10\%$ of the nominal voltage. Thus the voltage values are neglected from all of the analysis. Also the final $\mathbf{SoC}_{\mathrm{EV},n}$ are neglected as all of the charging strategies managed to charge the EVs till full battery before the following day's first journey. The simulation results displayed that none of the strategies violated the transformers maximum

capacity, which is 630 kVA as introduced in section 3.1.

In addition, the following parameters and methods are selected and used consistently throughout the simulations. The window size, for the moving window optimization, is of 16 hours and it is taken from the paper [38]. It represents a compromise value which provides reasonable results both with and without errors. As the optimization step is 15 minutes, the used household load profiles need to be compressed for the optimization process. The needed household load profiles are generated by sampling the original 1 minute resolution profiles with 15 minute steps for the needed optimization window size. This sampling causes a certain inaccuracy for the DBS, SBS and the CBS, which are using the household load profiles to generate the constraints for the optimization process. Thus some current limit violations may exist.

Moreover, the initial time limit for the solvers, introduced in section 2.6, is 10 seconds. In case this time turns out to be insufficient, it is increased in 40 second steps to the extend that a solution is found, as presented in Figure 6. The penalty factors, introduced in chapter 2, are from the parameter study presented in appendix D. Accordingly the given factors are scaled to match the used simulation resolution. The used penalty factors are $P_{\mathrm{P}} = 0.0025$ and $C_{\mathrm{P}} = 0.05$. Next the different case studies are introduced, correspondingly the results are presented and analyzed.

4.1 Comparison of Single Charging Strategies

This section analyzes the results attained from the simulations performed by using one charging strategy for the whole EV fleet. The results are presented by four tables representing the different EV penetration rates and different simulation days respectively. Each table presents simulation results for all of the charging strategies, introduced in chapter 2.

4.1.1 Wednesday, 75 % EV Penetration Rate

In terms of EV user comfort, the simulation results in Table 4.1 indicate that the CBS manages to reduce the total charging costs by 71.2%, which is 4.1% more than the SBS and only 1.8% less than the ABS. Also the DBS manages to reduce the total charging costs by 30.4%. However, the DBS results count 79 net interruptions, which is almost one charging interruption for every EV. Whereas the CBS results count minus 3 net interruptions and the SBS results count 16 net interruptions. In terms of time flexibility, the DBS provides the least amount of time, while both the CBS and SBS provide 3.4 hours, which is the most out of all charging strategies.

Moreover, in terms of electric network impacts the, results indicate that only the DBS and the SBS manages to avoid the current limit violations, while surprisingly the CBS is causing 1.3% current limit violation that last for 1 minute. However the UCS and the ABS are causing more substantial current limit violations both in magnitude and duration. Furthermore, the DBS provides 50% network loss reduction, while the CBS reduces them only by 27.3%.

The network loss reduction by the CBS is on the one hand 7.7% more than by the ABS, but on the other hand 8% less than by the SBS. When considering the

Table 4.1: Simulation results on Wednesday with 75% EV penetration rate

	Scenario:	UCS	ABS	DBS	SBS	CBS
EV user comfort	Total charging cost [€]	85.7	23.2	59.6	28.2	24.7
	Change of charging cost[%]	0	-73	-30.4	-67.1	-71.2
	Net number of interruptions	0	-13	79	16	-3
	Time flexibility [h]	12.1	2.6	1.5	3.4	3.4
Electrical network impacts	Maximum load [kVA]	346	427	287	287	287
	Maximum current [A]	348	441	257	250	288
	Violation magnitude [%]	22.4	55.2	0.0	0.0	1.3
	Violation duration [min]	8	32	0	0	1
	Change of network losses [%]	0.0	-19.6	-50.0	-35.3	-27.3
	Cost of network losses [€]	8.0	1.6	3.1	1.6	1.6

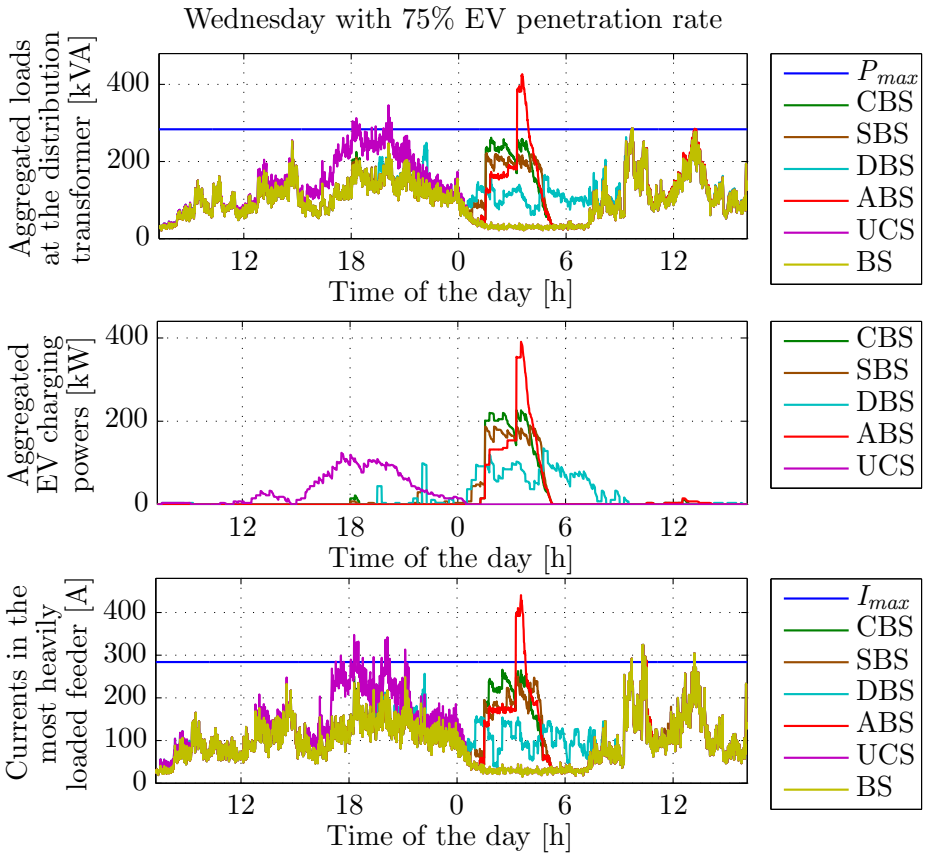

Figure 14: Wednesday, aggregated loads at the distribution transformer, aggregated EV charging powers and currents in the most heavily loaded feeder with 75% EV penetration rate

cost of network losses, the CBS comes out even with the SBS and ABS on 1.6 €, while the DBS would cause 1.5 € and the UCS 6.4 € higher cost for the network losses. Furthermore, Figure 14 presents the simulation results for the time when the EVs are charging.

Figure 14 indicates that the BS is already violating the I_{max}, which is the maximum current limit of the feeder cable. The P_{max} is the maximum power limit used by the DBS, SBS and the CBS. Moreover, this figure reveals the characteristics of each charging strategy. By the UCS, a large number of EVs are charging at 18:00 o'clock when the evening peak load hours begin. This causes the larges current limit violations in the UCS. On the other hand the SBS and the CBS are shifting the charging to low cost charging time. They also avoid the large current limit violations. Also whereas the DBS aims for valley filling, the ABS is concentrating the EV charging to 03:00 o'clock in the morning when the electricity price is clearly at a low level, as presented in section 3.4 in Figure 12. This causes 55% current limit violation which lasts for 32 minutes. The current limit violation in the CBS is not visible, as the BS is also causing current limit violations around the same time. The shapes of the aggregated EV charging powers remain similar as the EV penetration increases.

4.1.2 Wednesday, 100 % EV Penetration Rate

The results in Table 4.2 indicate that the total charging cost reduction by the CBS is still significant, even though it is 3.6% less than with 75% EV penetration rate. Here the CBS reduces the total charging costs by 67.6% which is 5.3% less than the ABS, yet still 7.1% more than the SBS. As mentioned in section 3.3, the EV user behaviors are randomly selected for each EV penetration rate.

Table 4.2: Simulation results on Wednesday with 100% EV penetration rate

	Scenario:	UCS	ABS	DBS	SBS	CBS
EV user comfort	Total charging cost [€]	105.1	28.5	67.3	41.5	34.1
	Change of charging cost[%]	0	-72.9	-36	-60.5	-67.6
	Net number of interruptions	0	-15	110	49	15
	Time flexibility [h]	12.4	2.9	2.3	3.7	3.7
Electrical network impacts	Maximum load [kVA]	353	538	287	287	287
	Maximum current [A]	396	549	285	283	293
	Violation magnitude [%]	39.5	93.1	0.4	0.0	3.1
	Violation duration [min]	12	49	1	0	1
	Change of network losses [%]	0.0	-3.7	-40.3	-33.9	-25.6
	Cost of network losses [€]	9.6	2.2	3.7	2.4	2.2

The net number of interruptions indicates the EV user behavior differences. Now also the CBS increases the net number of interruption to 15, while with 75% EV penetration rate it was minus 3. However, the CBS still causes 34 interruptions less than the SBS. On the time flexibility the CBS and the SBS provide 3.7 hour before the following day's first journey, which remains the most out of all strategies.

The increased EV penetration rate also causes clear changes to the electric network impacts. Here only the SBS manages to avoid the current limit violations while the DBS is causing a 0.4% current limit violation and the CBS is causing a 3.1% violation, both lasting for 1 minute. However, the UCS and the ABS are further

increasing the current limit violations both in magnitude and duration. Now the violation magnitude by the ABS is 93.1% lasting for 49 minutes.

In the network losses, the CBS provides 25.6% reduction, which is 8.3% less than the SBS and 14.7% less than the DBS. Even though in the network loss reduction the CBS performed worse than the SBS, in the cost of network losses the CBS and the ABS results in the smallest network loss costs of 2.2€, which is 0.2 € less than the SBS.

4.1.3 Saturday, 75 % EV Penetration Rate

The Saturday's EV energy demand is less than on Wednesday. The results, presented in Table 4.3, show that the total charging cost difference between the CBS and the SBS is considerably less than in either of the scenarios on Wednesdays. The CBS provides 62.6% total charging cost reduction which is only 1.9% more than SBS but on the other hand only 2.2% less than ABS. Moreover, the CBS results in minus 15 net interruptions, which is 2 less than the SBS, but 3 more than the ABS. Surprisingly the SBS provides the largest time flexibility, which is 1.7 hours more than the ABS, but only 0.4 hours more than the CBS and the DBS.

Table 4.3: Simulation results on Saturday with 75% EV penetration rate

	Scenario:	UCS	ABS	DBS	SBS	CBS
EV user comfort	Total charging cost [€]	40.6	14.3	26.6	16.0	15.2
	Change of charging cost[%]	0	-64.8	-34.6	-60.7	-62.6
	Net number of interruptions	0	-18	43	-13	-15
	Time flexibility [h]	18.0	4.0	5.3	5.7	5.3
Electrical network impacts	Maximum load [kVA]	308	288	267	267	267
	Maximum current [A]	324	307	216	207	251
	Violation magnitude [%]	14.1	8.2	0.0	0.0	0.0
	Violation duration [min]	1	26	0	0	0
	Change of network losses [%]	0.0	-11.7	-44.8	-28.8	-20.1
	Cost of network losses [€]	2.7	0.8	1.0	0.7	0.8

The results display that the maximum load by the households is less than on Wednesday. Here the DBS, SBS and the CBS manages to avoid all the current limit violations, which are occurring with the UCS and the ABS. The DBS still provides the largest network loss reduction by 44.8%, while the CBS reduces them by 20.1%, which is 8.7% less then SBS. However, when considering the costs of the network losses, the ABS and the CBS are even on 0.8 € while the SBS results in 0.1€ less, and the DBS causes 0.2 € higher costs to the network losses.

Figure 15 displays that the BS is not causing any current limit violations. Even though current limit violations occur with the UCS and the ABS, due to the same reason as on Wednesday. However, they are not as severe as on Wednesday due to the smaller EV energy demand. The difference between the EV user behavior on Wednesday and on Saturday is considerable. On Wednesday the UCS clearly concentrates the charging between 15:00 o'clock and 00:00 o'clock with a charging

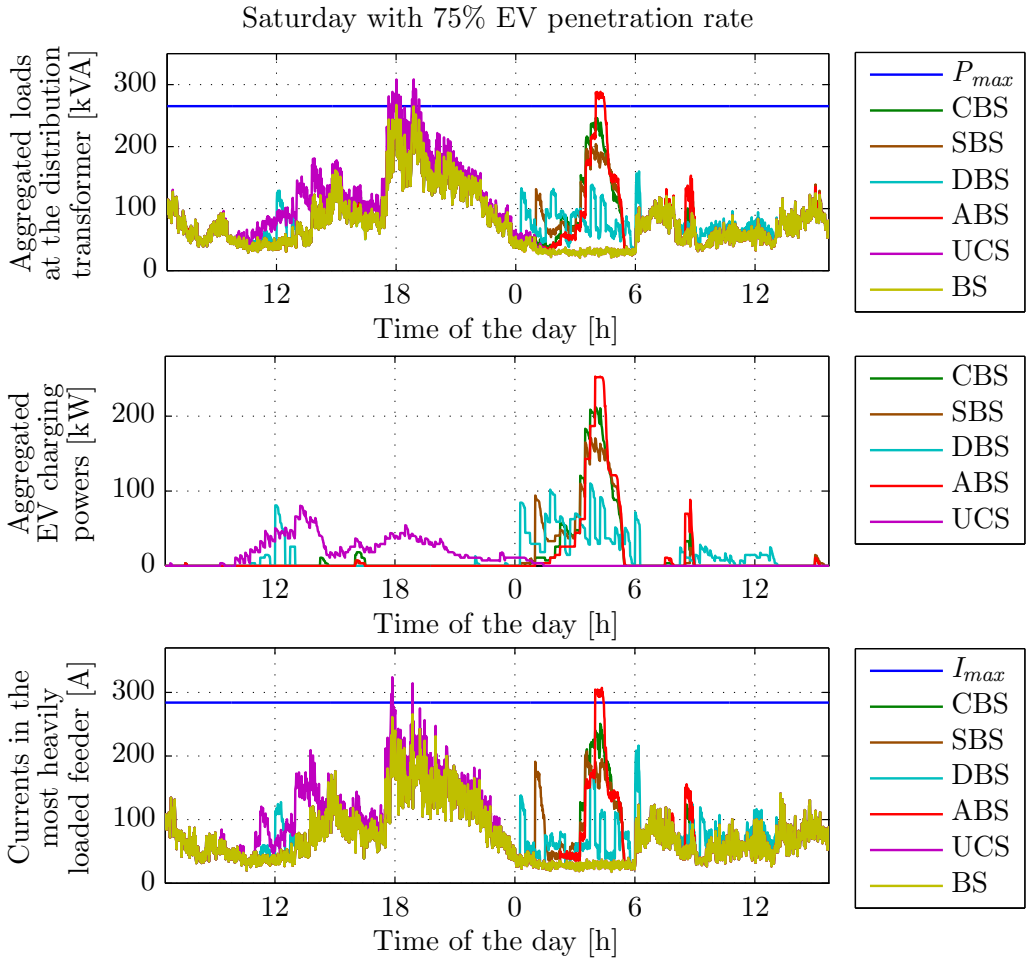

Figure 15: Saturday, aggregated loads at the distribution transformer, aggregated EV charging powers and currents in the most heavily loaded feeder with 75% EV penetration rate

peak at 18:00 o'clock, while on Saturday the charging starts already at 10:00 o'clock, peaks at 14:00 o'clock and continues over midnight. The other strategies aims the charging again to the night, where the load valley and electricity price valley exist. As the EV penetration rate increases, the increased energy demand by the EVs is elevating the aggregated EV charging power profiles accordingly. This means further violation magnitude and duration increments by the UCS and the ABS.

4.1.4 Saturday, 100 % EV Penetration Rate

Here the different user behaviors can be once again noticed. The results in Table 4.4 indicate that the CBS reduces the total charging costs by 55.9% which is only 0.4% less than the ABS and 3.7% more than the SBS. When the net number of interruptions is compared the ABS provides minus 20 net interruptions, while the CBS results in minus 1 and the SBS results in 9 net interruptions. However on time flexibility the CBS can provide only 6.5 hours, whereas the SBS provides 0.8 hours more and the ABS provides 1 hour more.

Moreover, the results with 100% EV penetration rate increases the difference in

Table 4.4: Simulation results on Saturday with 100% EV penetration rate

	Scenario:	UCS	ABS	DBS	SBS	CBS
EV user comfort	Total charging cost [€]	61.1	26.7	43.7	29.2	26.9
	Change of charging cost[%]	0	-56.3	-28.5	-52.2	-55.9
	Net number of interruptions	0	-20	86	9	-1
	Time flexibility [h]	17.9	7.5	5.7	7.3	6.5
Electrical network impacts	Maximum load [kVA]	356	311	267	267	267
	Maximum current [A]	374	323	275	234	272
	Violation magnitude [%]	31.8	13.8	0.0	0.0	0.0
	Violation duration [min]	5	48	0	0	0
	Change of network losses [%]	0.0	-8.9	-36.4	-32.4	-25.6
	Cost of network losses [€]	4.6	1.8	2.2	1.5	1.5

the electric network impacts between Wednesday and Saturday. On Wednesday the ABS causes the largest current limit violations in magnitude and duration, however on Saturday the UCS causes the largest current limit violations in magnitude while the ABS still causes the longest violation in duration. Here again the DBS, SBS and the CBS manage to avoid all the current limit violations. In the network losses the CBS results in 25.6% reduction which is 6.8% less than the SBS. The cost of network losses is the smallest by the CBS and the SBS, only 1.5 €, which is 0.3 € less than by the ABS and 0.7€ less than by the DBS.

4.1.5 Evaluation of Individual Charging Strategies

The results show that the developed charging strategy, the CBS, as well as the existing charging strategies, are behaving consistently. This is proven as the different days have totally different price profiles, household load profiles and EV user behaviors. The results show also that the CBS can provide significant total charging cost reductions in comparison to the UCS. The total charging cost reductions by the CBS are almost as much as by the ABS. The difference between the CBS and the charging cost wise „best case“ is in the range of 0.4% - 5.3%, while simultaneously the CBS avoids significant current limit violations, which the ABS perpetrates. The SBS results in 1.9% - 7.0% less charging cost reductions than the CBS, while avoiding all the current limit violations. The DBS results in 27.4% - 40.8% less charging cost reductions than the CBS. When considering the net number of interruptions and the time flexibility for the EVs the CBS proves to perform well. In most cases it manages to provide negative net interruptions and often offers one of the longest time flexibilities for the EVs.

Considering the electric network impacts, surprisingly only the SBS manages to perfectly avoid the current limit violations. However, the current limit violations can be explained by the inaccurate sampling of the used household load data, as explained earlier. The current limit violations with the DBS and the CBS could be avoided by taking the maximum loads from each simulation step to form the final household load profiles for the optimization process. In addition the current and

the voltage estimation inaccuracy could be taken into account with a larger safety margin. However, the DBS is the best strategy to provide network loss reductions. The CBS reduces the network losses by 20.1% - 27.3% while SBS reduces them with 6.8% - 8.7% more and the DBS with 10.8% - 24.8% more. However, the costs of the network losses are, in most cases, the smallest with the CBS. This is due to the fact that all of the network losses, the CBS causes, are concentrated to the times when the electricity prices are low. Therefore, the cost of the network losses would in fact increase the total charging cost difference between the CBS and other charging strategies making the CBS even more attractive. All of the three strategies, the DBS, SBS and the CBS, manage to avoid substantial current limit violations, which occur by the UCS and the ABS. Especially the ABS can not be considered realistically implementable, due to long lasting current limit violations of tens of percentage points.

4.2 Multiple EV Fleet Aggregators With Different Strategies

In this section, the simulation results acquired by sharing the EV fleet between two EV fleet aggregators, are evaluated. The results are presented in four bar charts per day. The results for the EV user comfort are presented in the 1st and 2nd charts and the electric network impact related results in the 3rd and 4th charts. The differences in charging cost, the net number of interruptions and the differences in network losses are computed in comparison to the results acquired by using the UCS for the whole EV fleet, as explained earlier. Each of the charts gather the different strategies into groups according to the applied share of EVs for the „Aggregator 1“. The different EV shares for the Aggregator 1 are 30%, 50%, 70% and 100% respectively. The 100% share repeats the results acquired by using single charging strategy for the whole EV fleet and they are used for comparison. Moreover, these aforementioned EV shares are forming different simulation scenarios named in Figure 16.

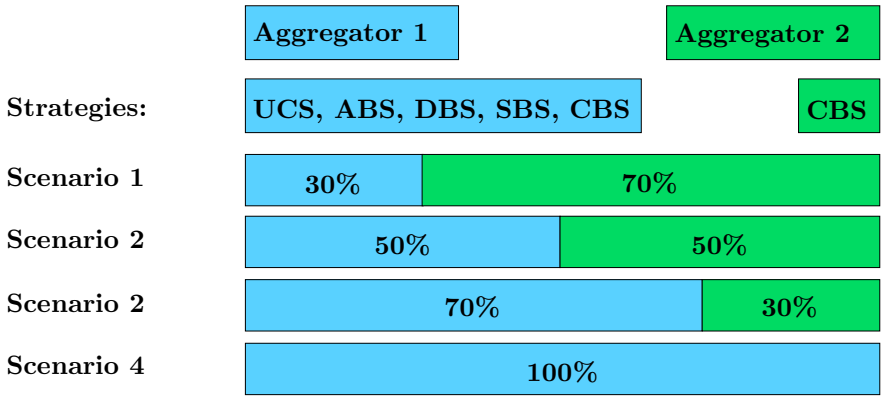

Figure 16: The share of EVs among the aggregators in different scenarios

It is also pointed out that the „Aggregator 2“ is always equipped with the CBS, while the Aggregator 1 is equipped with different strategies. The applied charging strategy combinations for the simulations are UCS-CBS, ABS-CBS, DBS-CBS,

SBS-CBS and CBS-CBS. Moreover, the presented results are summations of two individual EV fleet aggregators to compare their cumulative effects on the EV users' comfort and on the electric network impacts. In the charts, the bright colored bars represent the simulations performed with 75% EV penetration rate. The dark colored bars, which are extending some of the bars, present the difference simulating the same strategy combination with 100% EV penetration rate. Additionally, the DBS and the SBS are taking part in the capacity sharing explained in section 2.5.3. This is assumed because the DBS and the SBS also consider the electric network constraints which needs to be shared when multiple EV fleet aggregators are simulated. Otherwise the constraints would not comply with the real situation in the electric network, and electric network limit violations would be expected. Next, the simulation results are presented for Wednesday, following with the corresponding results for Saturday and finally the results are analyzed. Furthermore, the detailed results are presented by tables in appendix E.

4.2.1 Wednesday, Multiple EV Fleet Aggregators

First the results for the total charging cost and for the change of charging costs are presented in Figure 17.

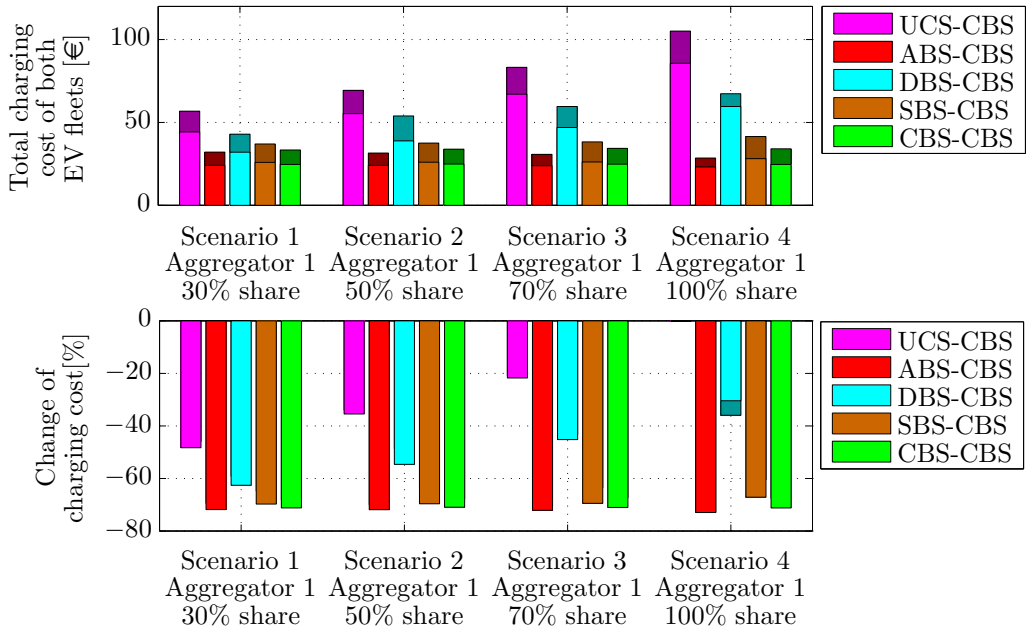

Figure 17: The total charging costs and the change percentage on Wednesday

The CBS manages to influence the UCS-CBS, DBS-CBS and the SBS-CBS combinations to reduce the total charging costs. In scenario 1 the influence of the CBS is the largest as it has 70% of the EVs. When the share gets smaller the influence decreases accordingly. However, in the ABS-CBS combination the influence of the CBS is almost negligible, yet still negative. This happens because the ABS performs better when it has all the EVs. Furthermore, the same influence of the CBS can be seen in the net number of interruption and time flexibility introduced in Figure 18.

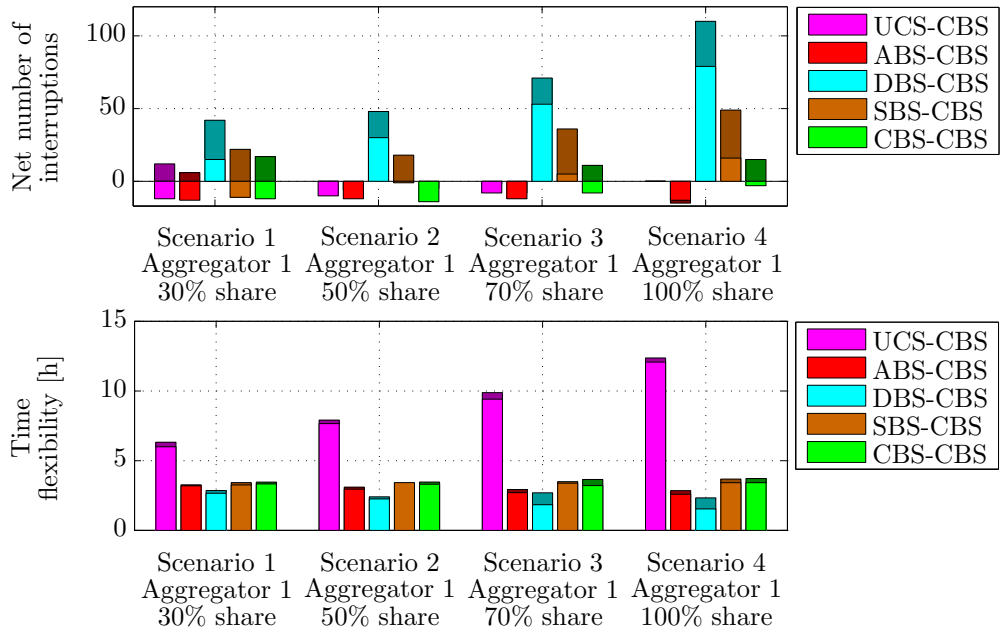

Figure 18: The net number of interruption and the time flexibility on Wednesday

The results indicate that the CBS has a positive influence on the net number of interruption, especially with 75% EV penetration rate. The results are negative in scenario 1 with 75% EV penetration rate with every charging strategy combinations except in the DBS-CBS. This happens because the DBS causes a considerable increase in interruptions, that the CBS is not able to mitigate. However, with 100% EV penetration rate the CBS increases the net number of interruptions in the UCS-CBS and the ABS-CBS combinations, while mitigating it in the DBS-CBS and the SBS-CBS combinations. As the share of EVs for the CBS gets smaller the positive influence for the DBS-CBS and the SBS-CBS combinations decreases. However, the CBS does not cause considerable changes to time flexibility in any of the charging strategy combinations. Only in the DBS-CBS combination does time flexibility increase to almost 3 hours in scenario 1, while in scenario 4, it is only 1.5 hours by the DBS. Next, the simulation results for the current limit violation magnitude and duration are presented in Figure 19.

In scenario 1 the CBS manages to mitigate the current limit violations happening in the UCS-CBS and the ABS-CBS combinations. However, as the UCS and the ABS gain a larger share of the EVs the current limit violations begin to increase. The results show interestingly that the CBS-CBS combination is not causing any current limit violations in scenario 1 and scenario 2. However, in scenario 3 the current limit violation exists. Moreover, the results for the changes of the network losses and the cost for the network losses are displayed in Figure 20.

In the DBS-CBS and the SBS-CBS combinations the network loss reductions are smaller when the CBS has larger share of the EVs. However, in the UCS-CBS and the ABS-CBS combinations the CBS manages to increase the network loss reduction. In scenario 1 the UCS-CBS combination results in a network losses reduction, which is higher than in the CBS in scenario 4. The same behavior is

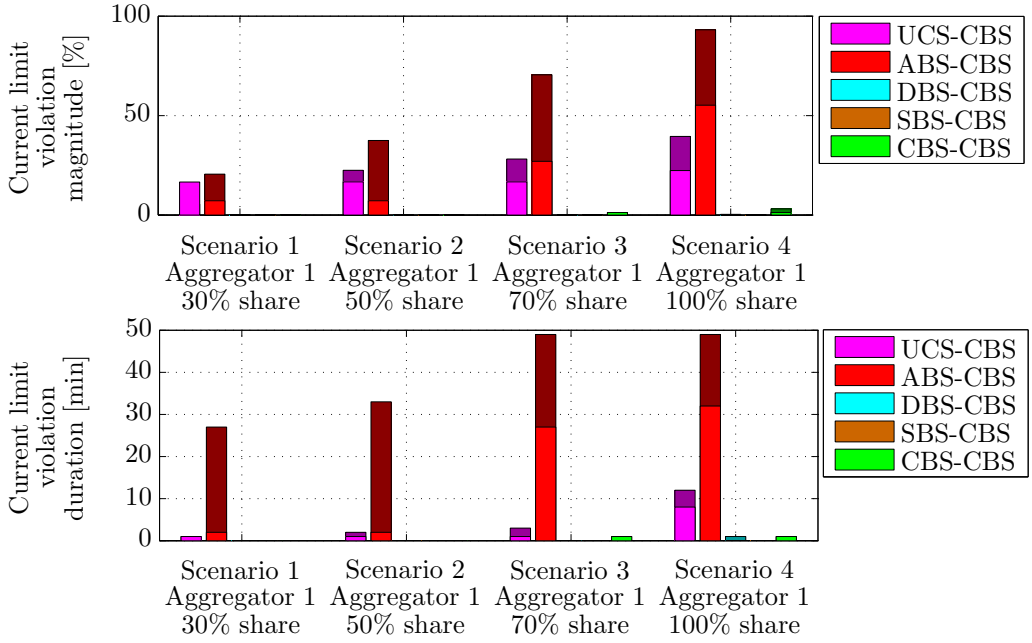

Figure 19: The current violation magnitude and duration on Wednesday

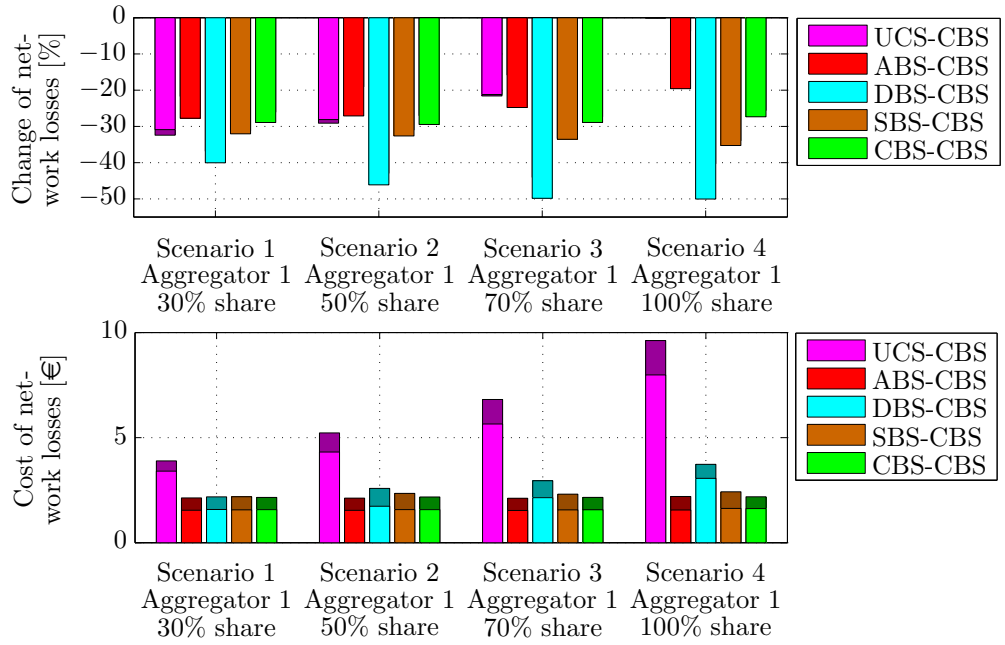

Figure 20: The costs and the changes of network losses on Wednesday

repeated with 100% EV penetration rate described by the darker bars. Moreover, the CBS reduces the cost for network losses in all charging strategy combinations, utmost in the UCS-CBS combination.

4.2.2 Saturday, Multiple EV Fleet Aggregators

The cost development in Figure 21 follows the same pattern seen in Wednesday's results. Surprisingly with 100% EV penetration rate the CBS manages to reduce the total charging costs in all charging strategy combinations.

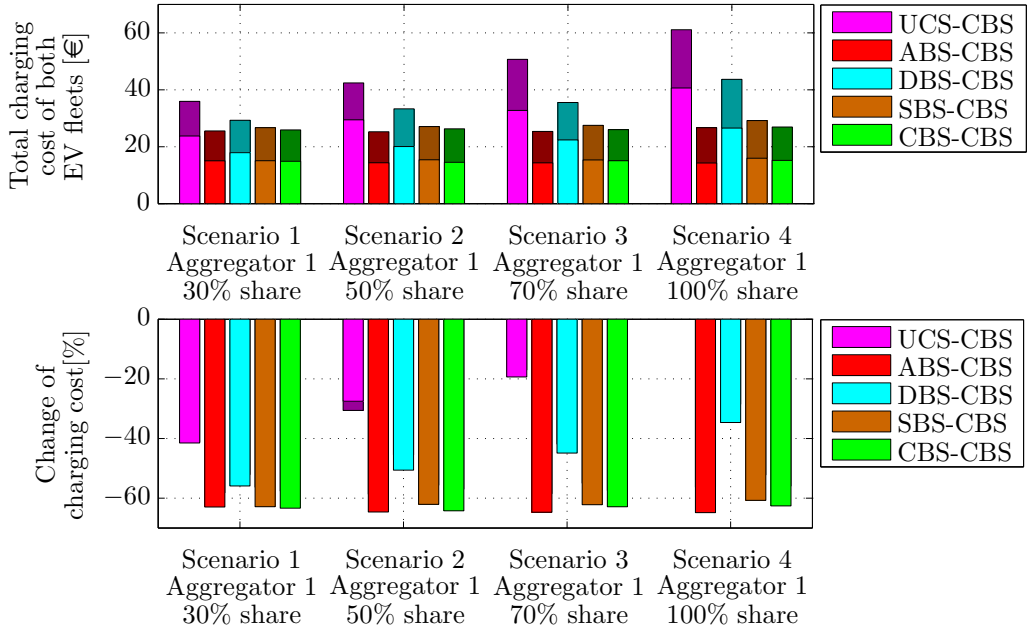

Figure 21: The total charging costs and the change percentage on Saturday

The ABS-CBS combination reaches the lowest total charging costs in scenario 2 where the EVs are shared evenly between the strategies. The charging cost reduction by the ABS-CBS combination in scenario 2 is 2.4% more than by the ABS in scenario 4. In scenario 1 the DBS-CBS combination almost reaches equally high cost reduction as the CBS in scenario 4.

Moreover, the results in Figure 21 present the net number of interruptions and time flexibility for Saturday. The ABS-CBS combination produce the smallest net number of interruptions in scenario 3, even though in scenarios 1 and scenario 2 the CBS is hindering the ABS ability to reduce charging interruptions. However, here the UCS-CBS, DBS-CBS and the SBS-CBS combinations perform better than the UCS, DBS and the SBS in scenario 4. However, in time flexibility the SBS-CBS combination performs worse in scenario 1, scenario 2 and scenario 3 than the SBS in scenario 4. This happens because the CBS provides less time flexibility than the SBS when they are both compared in scenario 4. The same can be observed in the ABS-CBS combination with 100% EV penetration rate.

Moreover, the CBS also manages to mitigate the current limit violations caused in the UCS-CBS and the ABS-CBS combinations, as displayed in Figure 23. In the ABS-CBS combination the current limit violations are totally avoided in scenario 1, scenario 2 and scenario 3 with 75% EV penetration rate. However, as the EV penetration rate increases the violations occur starting from scenario 1. In the UCS-CBS combination the current limit violations are only avoided in scenario 1 with 100% EV penetration rate.

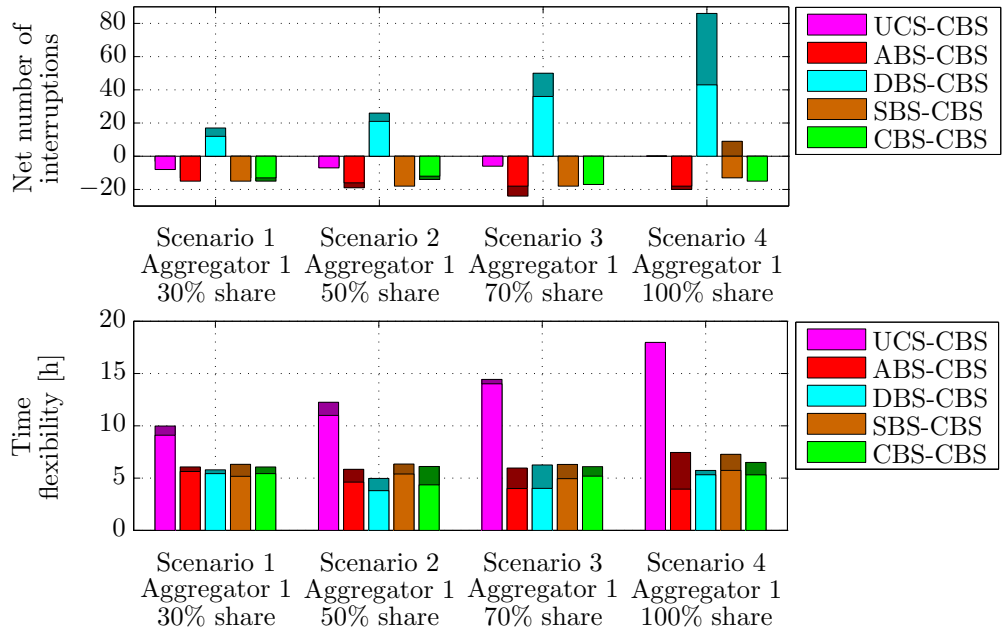

Figure 22: The net number of interruption and the time flexibility on Saturday

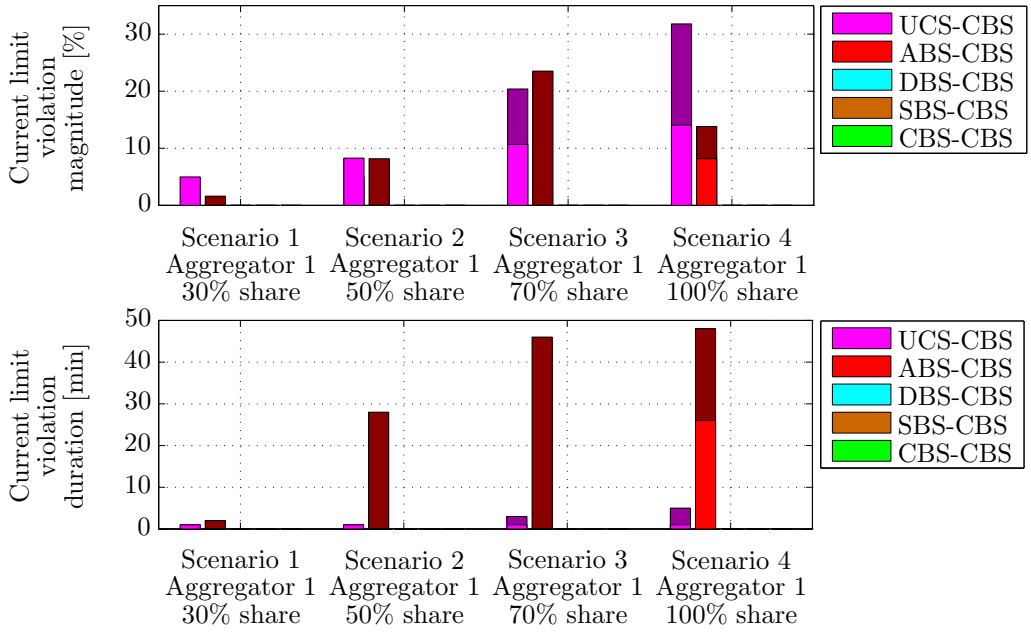

Figure 23: The current violation magnitude and duration on Saturday

The last results display the changes of network losses and the cost of the network losses in Figure 24. The UCS-CBS combination reaches almost the same level in the network loss reduction in scenario 1 as the SBS reaches in scenario 4. Also the cost of network losses in scenario 1 by the UCS-CBS combination is almost the same as the other combinations. Even though the network loss reductions are less in the DBS-CBS combination than the DBS in scenario 4, the DBS-CBS combination results in smaller or equal cost of network losses in scenario 1 and scenario 2 as the

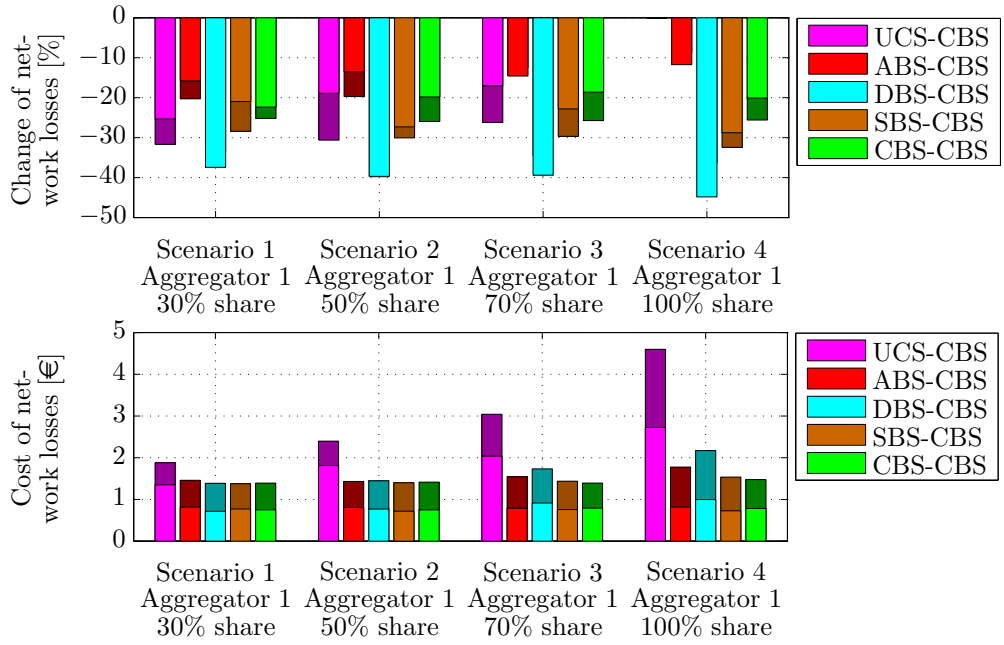

Figure 24: The costs and the changes of network losses on Saturday

CBS in scenario 4.

4.2.3 Evaluation of Multi Aggregator results

When considering the strengths of each individual strategy, they perform better alone than when they are sharing the EVs with the CBS. In EV user comfort, as a whole the CBS caused adverse effects in the ABS-CBS combination. This could be expected based on the results received by the single charging strategies, where the ABS performed better than the CBS in reducing the total charging costs and providing negative net number of interruptions. However, the CBS managed to increase the EV user comfort in the UCS-CBS, DBS-CBS and the SBS-CBS combinations by reducing the total charging costs and by decreasing the net number of interruptions.

The effects are similar when considering the effects to electric network impacts. The CBS managed to mitigate the negative electric network impacts in the UCS-CBS and the ABS-CBS combinations, but hindered the DBS's ability to reduce the network losses in the DBS-CBS combination. This was also expected as the DBS performed better alone in network loss reduction than the CBS. However, the CBS managed to reduce the costs of the network losses in almost all of the charging strategy combinations and scenarios. This occurred because the CBS caused the network losses when the electricity prices are low.

Furthermore, the result indicates that the dual EV fleet aggregator equipped with CBS-CBS combination performs better than the single CBS in scenario 4. This can be explained by the random assignment of the EVs for each EV fleet aggregator and the used optimization environment. The difference is noticeable in the net number of interruptions and higher charging cost reductions. As long as the

„difficult“ scheduling cases are allocated to the EV fleet aggregator which has the smaller share of the EVs, the combined result is „ideal“. However, as the share of EVs changes and ultimately comes to be optimized by only one EV fleet aggregator, the found result's can be seen to differ from the „ideal“. This is understandable as the two EV fleet aggregators have twice as much time for their optimization problem compared to one EV fleet aggregator, as introduced in section 2.5.3.

The results indicate that the UCS-CBS and the ABS-CBS combinations would cause current limit violations to the electric network even in scenario 1, where only 30% of the EVs would be charged in either uncontrolled manner or purely based on charging cost minimization. However, the DBS-CBS, SBS-CBS and the CBS-CBS would be possible combinations as they avoid severe current limit violations. However, the EVs which are not represented by the CBS or the SBS would be facing high charging costs. Also they would be accountable for the higher cost of network losses.

Chapter 5

Summary, Conclusion and Future Research

5.1 Summary of the Work

First, the need for the controlled EV charging is explained. Moreover, the complexity related to the realistic EV charging control implementation is introduced. Then earlier publications are reviewed in order to acquire new ideas and to derive the existing strategies to evaluate the new charging strategy. After which the related problem for this thesis is stated, ideas to solve it presented and the differences to earlier publications explained.

Furthermore, the existing strategies are introduced and the new charging strategy is developed. For each strategy the expected behavior is discussed, main objective function is defined and the related mathematical optimization problems are formulated. In addition, the multi EV fleet aggregator implementation with relaxed DSO - EV fleet aggregator communication is developed. Also the optimization environment is presented and the moving window optimization is introduced.

Subsequently the test environment for the new charging strategy is developed. The electric network model is simulated by ePHASORsim solver [40] enabling the on-line simulations. The used model represents a German suburban LV-network for which the details are taken from the dissertation [42]. Moreover, the vectorized EV model, sourced from [10], is tuned to present the charging behavior of Mitsubishi iMiEV. The data for EV user behavior is generated from a surveyed dataset collected in [43]. The household load profiles are based on German statistics and received from [45]. The historical intra-day price profiles are taken from the EPEX spot market database [46]. Also the work flow of the main algorithm, explaining the simulation and optimization steps, is presented.

Subsequently, the used parameter settings and methods for the simulation work are presented. Then the performance of the new charging strategy is evaluated based on various different simulation scenarios. Firstly, the simulation results are presented and evaluated for single charging strategies for Wednesday and Saturday with two different EV penetration rates respectively. Secondly, the results attained by simulations with multiple EV fleet aggregators are presented and evaluated. On the evaluation the focus is kept on EV users' comfort and electric network impact related aspects.

5.2 Conclusion

As shown in section 2.5, a new charging strategy for realistic implementation has been developed. The EV users comfort and close to perfect electric network friendliness is demonstrated and evaluated on realistic simulation scenarios against three

existing charging strategies and a uncontrolled charging scenario, compared in chapter 4.

The results indicate that the new charging strategy can produce considerable charging cost savings for the EV users in comparison to the uncontrolled charging. The total charging costs saving by the new charging strategy are 55.9% - 71.2%, which are 1.9% - 7.0% more than by the main competitor SBS. Even though, the new charging strategy was found to cause higher network losses than the SBS, the new charging strategy resulted in smaller costs for network losses.

In addition, multiple EV fleet aggregator scenarios were simulated by having the new strategy always as the second strategy. The new charging strategy reduced the total charging costs by 2.1% - 4.3% when combined with the SBS. Furthermore, the new charging strategy was found to increase the network losses by 3% - 7% when combined with the SBS. However, the corresponding costs for the network losses were equal to or smaller than by the SBS in single strategy results.

The observed current limit violations by the new charging strategy and the DBS were found to be caused by the sampling method used to generate household load profiles for the optimization process. The simulations for the new charging strategy were repeated for the single charging strategy scenarios where the current violations existed. The new sampling method, discussed in section 4.1.5, provides results where the current limit violations are avoided. The received results with 75% EV penetration rate on Wednesday show 24.9 € total charging cost, which is 71% cost reduction in comparison to the UCS. This result is only 0.2% less than the old one. The cost of network losses by the new simulation are 1.6 €, which is the same as by the old one. With 100% EV penetration rate the total charging cost is 35.1 €, which means 66.6% cost reduction. The new result is 1.0% less than the old one. The costs for network losses, however are 2.2 €, which is also the same than the old one.

Furthermore, the new charging strategy was motivated by the traffic light concept. The new charging strategy can be seen to work on range of the green phase and the amber phase. As introduce in the traffic light concept, also in the new charging strategy the DSO is determining the current and forecast condition of the electric network. Here the conditions are specified by a technical signal. The results show that the technical signal used for communication between the DSO and the EV fleet aggregator is robust, to account for electric network limitations. On the other hand, it gives the scheduling flexibility for the EV fleet aggregator to optimize the charging profiles based on cost. In single charging strategy scenario, the used communication works without iteration and when multiple EV fleet aggregator are involved, one additional iteration is sufficient. As long as the forecast data is accurate for the DSO to calculate the power capacity profiles, all the electric network violations can be avoided. Moreover, the results indicate the new strategy has potential for further development.

5.3 Future Research

In this thesis the performance of the new charging strategy is evaluated based on various different simulation scenarios. However, there are still a few point which

could not be covered due to the limited time available for this thesis. Therefore, they could be addressed in future research:

- Enhance the DSO's calculations to be updated during the operation to increase the current and the voltage estimation safety margin in case further violations occur.
- More comprehensive tests and evaluations should be performed in various realistic electric network models
- The household load profiles should be taken from different seasons of the year
- Larger variety of different EV penetration rates should be used
- The V2G capability could be incorporated into the new charging strategy. In addition to the capacity profiles, the DSO could also issue demand profiles and a purchasing price profile. The demand profiles would include the feeder wise demands in addition to the global demand profile. The purchasing price profile specifies how much the DSO is willing to pay for the electricity fed back to the electric network. Based on the demand and purchasing price profiles, the EV fleet aggregator could perform the trade-off calculations. Based on these calculations the V2G regulation would be performed. However, this would require more assumptions related battery aging to find a proper tariff scheme to motivate EV users into such arrangements.
- The communication signal between the DSO and the EV fleet aggregator could be changed into a cost signal, which would be added into the price profile used by the new charging strategy, as proposed by [33]. The Use-of-System tariff is also proposed earlier for distributed generation by [48] and [49] and a similar arrangement is proposed for other retail electricity customers by [50].

Bibliography

[1] BMWI. Energie in deutschland, trends und hintergrnde zur energieversorgung. [Online]. Available: „`http://www.bmwi.de/`“ February 2013. [Accessed 21.4.2015].

[2] U.S. Department of Energy. All-electric vehicles. [Online]. Available: „`https://www.fueleconomy.gov/feg/evtech.shtml`“ [Accessed 12.5.2015].

[3] J. de Hoog, D.A. Thomas, V. Muenzel, D.C. Jayasuriya, T. Alpcan, M. Brazil, and I. Mareels. Electric vehicle charging and grid constraints: Comparing distributed and centralized approaches. In *Power and Energy Society General Meeting (PES), 2013 IEEE*, pages 1–5, July 2013.

[4] S. Shafiee, M. Fotuhi-Firuzabad, and M. Rastegar. Investigating the impacts of plug-in hybrid electric vehicles on power distribution systems. *Smart Grid, IEEE Transactions on*, 4(3):1351–1360, Sept 2013.

[5] A.S. Masoum, S. Deilami, P.S. Moses, M.A.S. Masoum, and A. Abu-Siada. Smart load management of plug-in electric vehicles in distribution and residential networks with charging stations for peak shaving and loss minimisation considering voltage regulation. *Generation, Transmission Distribution, IET*, 5 (8):877–888, August 2011.

[6] K. Mets, T. Verschueren, W. Haerick, C. Develder, and F. De Turck. Optimizing smart energy control strategies for plug-in hybrid electric vehicle charging. In *Network Operations and Management Symposium Workshops (NOMS Wksps), 2010 IEEE/IFIP*, pages 293–299, April 2010.

[7] S.M.M. Agah and A. Abbasi. The impact of charging plug-in hybrid electric vehicles on residential distribution transformers. In *Smart Grids (ICSG), 2012 2nd Iranian Conference on*, pages 1–5, May 2012.

[8] A.P. Azad, O. Beaude, s. Lasaulce, and L. Pfeiffer. An optimal control approach for ev charging with distribution grid ageing. In *Communications and Networking (BlackSeaCom), 2013 First International Black Sea Conference on*, pages 206–210, July 2013.

[9] H. Turker, S. Bacha, and A. Hably. Rule-based charging of plug-in electric vehicles (pevs): Impacts on the aging rate of low-voltage transformers. *Power Delivery, IEEE Transactions on*, 29(3):1012–1019, June 2014.

[10] Chenjie Ma, F. Marten, J.-C. Tobermann, and M. Braun. Evaluation of modeling and simulation complexity on studying the impacts of electrical vehicles fleets in distribution systems. In *Power Systems Computation Conference (PSCC), 2014*, pages 1–7, Aug 2014.

[11] M.D. Galus, C. Dobler, R. A. Waraich, and G. Andersson. Predictive, distributed, hierarchical charging control of phevs in the distribution system of a large urban area incorporating a multi agent transportation simulation. Technical report, ETH, Eidgenössische Technische Hochschule Zrich, IVT, Institut fr Verkehrsplanung und Transportsysteme, 2011.

[12] R.A Verzijlbergh, M.O.W. Grond, Z. Lukszo, J.G. Slootweg, and M.D. Ilic. Network impacts and cost savings of controlled ev charging. *Smart Grid, IEEE Transactions on , vol.3*, pages 1203–1212, 2012.

[13] L. Pieltain Fernández, T.G.S. Román, R. Cossent, C.M. Domingo, and P. Frías. Assessment of the impact of plug-in electric vehicles on distribution networks. *Power Systems, IEEE Transactions on , vol.26*, pages 206–213, 2011.

[14] U.C. Chukwu and S.M. Mahajan. Real-time management of power systems with v2g facility for smart-grid applications. *Sustainable Energy, IEEE Transactions on*, 5(2):558–566, April 2014.

[15] Tan Ma and O.A. Mohammed. Economic analysis of real-time large-scale pevs network power flow control algorithm with the consideration of v2g services. *Industry Applications, IEEE Transactions on*, 50(6):4272–4280, Nov 2014.

[16] BDEW. Bdew roadmap, realistic steps for the implementation of smart grids in germany. Technical report, The German Association of Energy and Water Industries, 2013.

[17] N. Rotering and M. Ilic. Optimal charge control of plug-in hybrid electric vehicles in deregulated electricity markets. *Power Systems, IEEE Transactions on , vol.26*, pages 1021–1029, 2011 2011.

[18] Zhongjing Ma, D. Callaway, and I. Hiskens. Decentralized charging control for large populations of plug-in electric vehicles: Application of the nash certainty equivalence principle. In *Control Applications (CCA), 2010 IEEE International Conference on*, pages 191–195, Sept 2010.

[19] K. Xie, L. Dong, X. Liao, Z. Gao, and Y. Gao. Game-based decentralized charging control for large populations of electric vehicles. *Przeglad Elektrotechniczny (Electrical Review)*, pages 252–256, 2012.

[20] Zhongjing Ma. Decentralized valley-fill charging control of large-population plug-in electric vehicles. In *Control and Decision Conference (CCDC), 2012 24th Chinese*, pages 821–826, May 2012. doi: 10.1109/CCDC.2012.6244126.

[21] Wenbo Shi and V.W.S. Wong. Real-time vehicle-to-grid control algorithm under price uncertainty. In *Smart Grid Communications (SmartGridComm), 2011 IEEE International Conference on*, pages 261–266, Oct 2011.

[22] Yifeng He, B. Venkatesh, and Ling Guan. Optimal scheduling for charging and discharging of electric vehicles. *Smart Grid, IEEE Transactions on*, 3(3): 1095–1105, Sept 2012.

[23] J. Rivera, P. Wolfrum, S. Hirche, C. Goebel, and H.-A. Jacobsen. Alternating direction method of multipliers for decentralized electric vehicle charging control. In *Decision and Control (CDC), 2013 IEEE 52nd Annual Conference on*, pages 6960–6965, Dec 2013.

[24] P. Richardson, D. Flynn, and A. Keane. Local versus centralized charging strategies for electric vehicles in low voltage distribution systems. *Smart Grid, IEEE Transactions on*, 3(2):1020–1028, June 2012.

[25] E. Sortomme, M.M. Hindi, S.D.J. MacPherson, and S.S. Venkata. Coordinated charging of plug-in hybrid electric vehicles to minimize distribution system losses. *Smart Grid, IEEE Transactions on , vol.2*, pages 198–205, 2011.

[26] K. Clement-Nyns, E. Haesen, and J. Driesen. The impact of charging plug-in hybrid electric vehicles on a residential distribution grid. *Power Systems, IEEE Transactions on , vol.25*, pages 371–380, 2010.

[27] Zhenpo Wang and Shuo Wang. Grid power peak shaving and valley filling using vehicle-to-grid systems. *Power Delivery, IEEE Transactions on , vol.28*, pages 1822–1829, 2013 2013.

[28] Peng Zhang, Kejun Qian, Chengke Zhou, B.G. Stewart, and D.M. Hepburn. A methodology for optimization of power systems demand due to electric vehicle charging load. *Power Systems, IEEE Transactions on*, 27(3):1628–1636, Aug 2012.

[29] O. Sundström and C. Binding. Flexible charging optimization for electric vehicles considering distribution grid constraints. *Smart Grid, IEEE Transactions on, vol.3*, pages 26–37, 2012 2012.

[30] A. O'Connell, D. Flynn, and A. Keane. Rolling multi-period optimization to control electric vehicle charging in distribution networks. *Power Systems, IEEE Transactions on*, 29(1):340–348, Jan 2014.

[31] M.F. Shaaban, M. Ismail, E.F. El-Saadany, and Weihua Zhuang. Real-time pev charging/discharging coordination in smart distribution systems. *Smart Grid, IEEE Transactions on*, 5(4):1797–1807, July 2014.

[32] P. Mahat, M. Handl, K.R. Kanstrup, A.P. Lozano, and A. Sleimovits. Price based electric vehicle charging. In *Power and Energy Society General Meeting, 2012 IEEE*, pages 1–8, July 2012.

[33] I. Momber, T. Gomez, and L. Soder. Pev fleet scheduling with electricity market and grid signals charging schedules with capacity pricing based on dso's long run marginal cost. In *European Energy Market (EEM), 2013 10th International Conference on the*, pages 1–8, May 2013.

[34] Inc. CVX Research. CVX: Matlab software for disciplined convex programming, version 2.0. [Online]. Available: „`http://cvxr.com/cvx`“ Aug 2012. [Accessed 20.3.2015].

[35] M. Grant and S. Boyd. Graph implementations for nonsmooth convex programs. In V. Blondel, S. Boyd, and H. Kimura, editors, *Recent Advances in Learning and Control*, Lecture Notes in Control and Information Sciences, pages 95–110. Springer-Verlag Limited, 2008.

[36] ApS Mosek. *The MOSEK optimization toolbox for MATLAB manual. Version 7.1 (Revision 28).*, 2015.

[37] Optimization Inc. Gurobi. Gurobi optimizer reference manual. [Online]. Available: „`http://www.gurobi.com`“ April 2015. [Accessed 23.4.2015].

[38] Chenjie Ma, J. Rautiainen, D. Dahlhaus, A. Lakshman, J.-C. Tobermann, and M. Braun. Efficient charging strategies of electric vehicles for future grids. In *9th International Renewable Energy Storage Conference and Exhibition (IRES 2015)*, pages 1–11, Feb 2015.

[39] MATLAB. *version 7.13.0 (R2011b)*. The MathWorks Inc., Natick, Massachusetts, United States, 2011.

[40] OPAL-RT. ephasorsim brochure. [Online]. Available: „`http://www.opal-rt.com`“ 2013. [Accessed 13.3.2015].

[41] A. Lakshman. Comparison of grid-supportive charging strategies for electric vehicles based on realistic mobility data. Master's thesis, RWTH Aachen University, December 2014.

[42] G. Kerber. *Aufnahmefähigkeit von Niederspannungsverteilnetzen für die Einspeisung aus Photovoltaikkleinanlagen*. PhD thesis, Technische Universität München, 2011.

[43] MiD. Mobilität in deutschland 2008. Technical report, infas Institute for Applied Social Sciences, German Aerospace Center (DLR) and Federal Ministry of Transport, Building and Urban Development (BMVBS), 2008.

[44] Mitsubishi-Motors. Mitsubishi imiev brochure. [Online]. Available: „`http://www.mitsubishi-cars.co.uk`“ 2015. [Accessed 16.3.2015].

[45] J. v. Appen, J. Haack, and M. Braun. Erzeugung zeitlich hochaufgelöster stromlastprofile für verschiedene haushaltstypen. In *Erzeugung zeitlich hochaufgelöster Stromlastprofile für verschiedene Haushaltstypen*, 2014.

[46] European Power Exchange. Epex spot. [Online]. Available: „`http://www.epexspot.com`“ 2015. [Accessed 28.4.2015].

[47] BDEW. Bdew-strompreisanalyse märz 2015. [Online]. Available: „`https://www.bdew.de/internet.nsf/id/preise-de`“ March 2015. [Accessed 24.3.2015].

[48] A. González and T. Gómez. Use of system tariffs for distributed generators. In *Power Systems Computation Conference (PSCC), 2008*, pages 1–7, July 2008.

[49] Chenghong Gu and Furong Li. Long-run marginal cost pricing based on analytical method for revenue reconciliation. *Power Systems, IEEE Transactions on*, 26(1):103–110, Feb 2011.

[50] Huang Hai-tao, Zhang Li-zi, Chen Yu, and Qiao Hui-ting. The capacity cost allocation model for retail electricity customers considering load patterns. In *Industrial Electronics and Applications (ICIEA), 2011 6th IEEE Conference on*, pages 45–50, June 2011.

[51] R.D. Zimmerman, C.E. Murillo-Sánchez, and R.J. Thomas. Matpower: Steady-state operations, planning, and analysis tools for power systems research and education. *Power Systems, IEEE Transactions on*, 26(1):12–19, Feb 2011.

[52] S. Kitano, K. Nishiyama, J.-i. Toriyama, and T. Sonoda. Development of large-sized lithium-ion cell „'lev50'“ and its battery module „'lev50-4'“ for electric vehicle. Technical report, GS Yuasa, -, 2008.

[53] F. Marten. Modellvalidierung (internal document). Technical report, Fraunhofer IWES, Kassel, 2013.

[54] M. Broussely, Ph. Biensan, F. Bonhommeb, and Ph. Blanchard. Main aging mechanisms in li ion batteries. *Journal of Power Sources*, pages 90–96, 2005.

Appendix A

Voltage and Current Estimation

To implement the new charging strategy in a reliable manner, the electric network sensitivities, voltage changes and current congestion due to EV charging need to be estimated. To estimate these variables a power system bus admittance matrix $\mathbb{Y}_{\text{bus}}$ and a Jacobian matrix $\mathbb{J}$ are examined. These matrices are used to estimate the node voltages and the line currents based on a forecast household load data. To build these matrices, a certain knowledge of the electric network is needed, i.e. network topology, line impedances/admittances, nominal voltages and loads. Four different constant comparison points are calculated from the used data, and the estimation errors produced by them are analyzed. Based on the results, a reliable comparison point is proposed. In the next part, the used data and the methods are explained and results and recommendations are presented.

A.1 Data and Methods

The electric network model, introduced in section 3.1, is used to study and develop the current and voltage estimation for the new charging strategy. Based on the electric network details the $\mathbb{Y}_{\text{bus}}$ and the $\mathbb{J}$ matrices are generated by MatPower[51]. The household load profile from the chosen Wednesday, introduced in section 3.4, is used. From the given profile, 20 time steps, representing a 5 hour peak loading time period from 15:00 till 20:00 with 15 minute resolution, are taken. MatPower is used to calculate the accurate voltages and current flows in the electric network. These results are used as „real measurement“ values against which the estimations results are analyzed. To estimate the future voltages and currents in a consistent manner, constant comparison values for the active power P_{comp} and the reactive power Q_{comp} are examined. They are used to calculate the active power difference $\mathbf{\Delta P}$ and the reactive power difference $\mathbf{\Delta Q}$ which are further used in the voltage and current estimation. The equation to calculate the power differences can be derived as $\mathbf{\Delta P} = \mathbf{P}_{\text{hh},h,\tau} - P_{\text{comp}}$ and $\mathbf{\Delta Q} = \mathbf{Q}_{\text{hh},h,\tau} - Q_{\text{comp}}$. The comparison point powers are taken from the data as maximum load, mean load, median load, and zero load case. The equation for the voltage estimation is as follows:

$$\begin{bmatrix} \Delta\delta \\ \mathbf{\Delta V} \end{bmatrix} = \mathbb{J}^{-1} \cdot \begin{bmatrix} \mathbf{\Delta P} \\ \mathbf{\Delta Q} \end{bmatrix} = \begin{bmatrix} \frac{\partial\delta}{\partial P} & \frac{\partial\delta}{\partial Q} \\ \frac{\partial V}{\partial P} & \frac{\partial V}{\partial Q} \end{bmatrix} \cdot \begin{bmatrix} \mathbf{\Delta P} \\ \mathbf{\Delta Q} \end{bmatrix}, \tag{A.1.1}$$

where $\mathbb{J}^{-1}$ is the inverse of the Jacobian matrix, and it is opened with its partial derivatives on the right hand-side of the equation. From the voltage angle difference $\Delta\delta$ and voltage magnitude difference $\mathbf{\Delta V}$, the complex form voltage $\Delta\mathbb{V}$ is formulated and used as shown in the following equation:

$$\Delta\mathbb{I} = \mathbb{Y}_{\text{bus}} \cdot \Delta\mathbb{V}, \tag{A.1.2}$$

where $\Delta\mathbb{I}$ is the complex current difference. Four estimation runs are performed and estimation values are stored and analyzed with reference to the real measurement values.

A.2 Results

From the first estimation results it can be seen that depending on the comparison point, the estimation results are different. Figure 25 show the results of the voltage and current estimations.

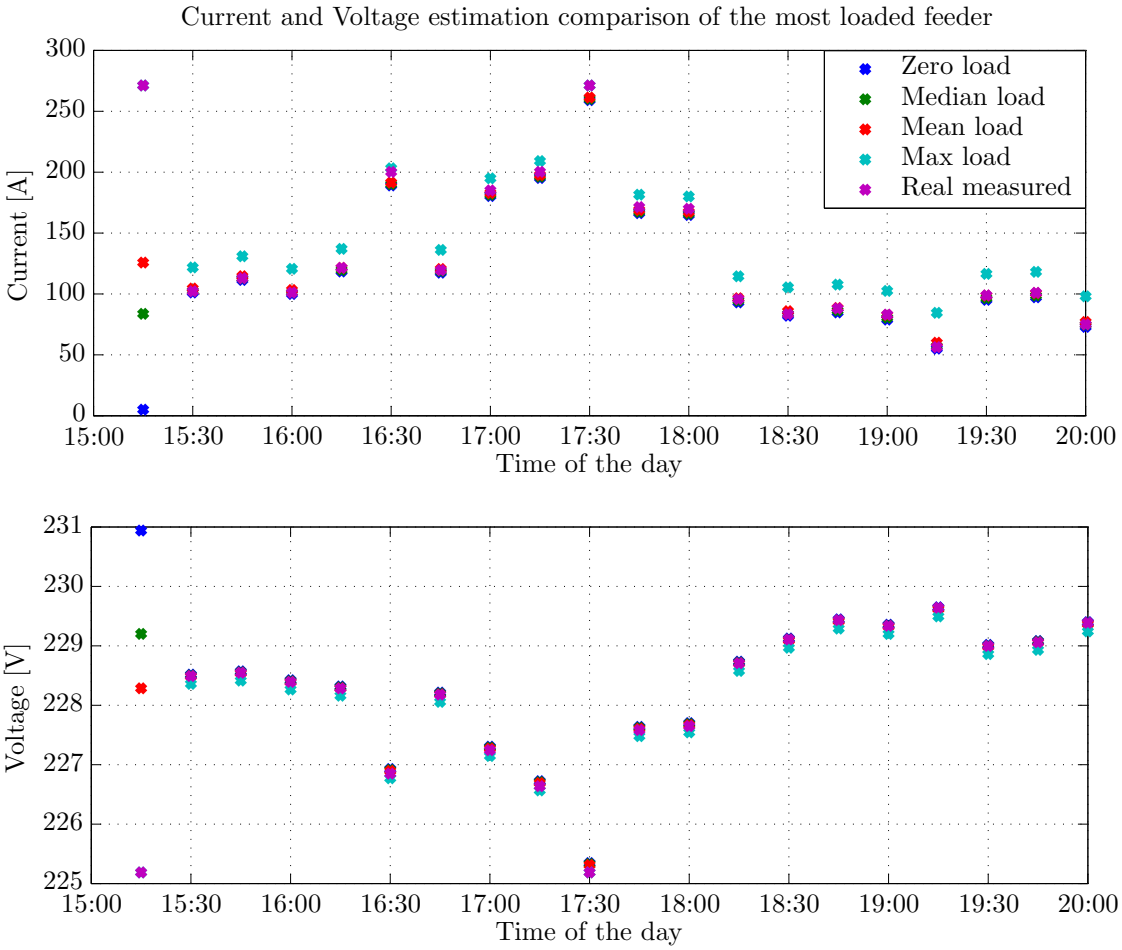

Figure 25: Voltage and current estimation

The estimation results are differ from each other because the load flow equations are not solved iteratively in order to save time. When the forecast power values differ a lot from the constant comparison point, the estimation results are inaccurate. Despite of this, the voltage errors are negligible small. The maximum voltage estimation error in all of the four cases is $\pm$ 0.07 %. However, the current estimation is more inaccurate. The current estimation error for the zero load is +0% -5.5%, for the median load +1.3% -5.0%, for the mean load +6.5% -4.3% and for the maximum load +50% -0%. The results in Figure 26 show that in maximum load case the

estimated currents are always more than the real measured currents, except when the comparison point is close to than of the forecast load. A vice versa effect is seen for the zero load case currents.

A.3 Recommendations

Based on this study, the zero load case is proposed to be taken as a constant comparison point for the voltage and current estimation. It results an accuracy of +0% -5.5% in the current and ± 0.07 % in the voltage estimations. Based on the proposed constant comparison point, the reference voltage $\mathbb{V}_{\text{ref},m}$ and the reference current $\mathbb{I}_{\text{ref},l}$ can be calculated. They are used for the voltage and current constraints in equations (2.3.3) and (2.3.4). This is seen to be the most accurate of the studied cases. It is recommended that the received error is compensated in the constraint calculation to avoid current and voltage limit violations.

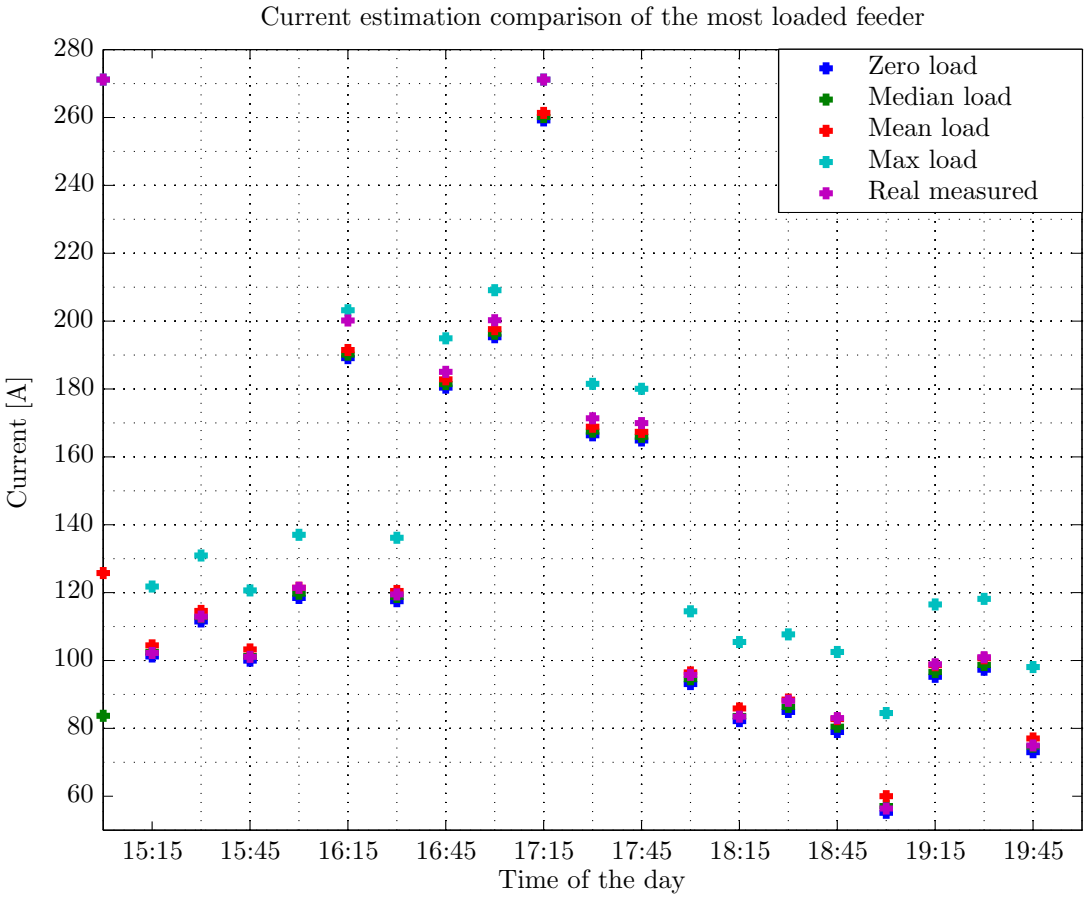

Figure 26: Current estimation

Appendix B

Detailed Flowchart for Multi EV Fleet Aggregator Scenario

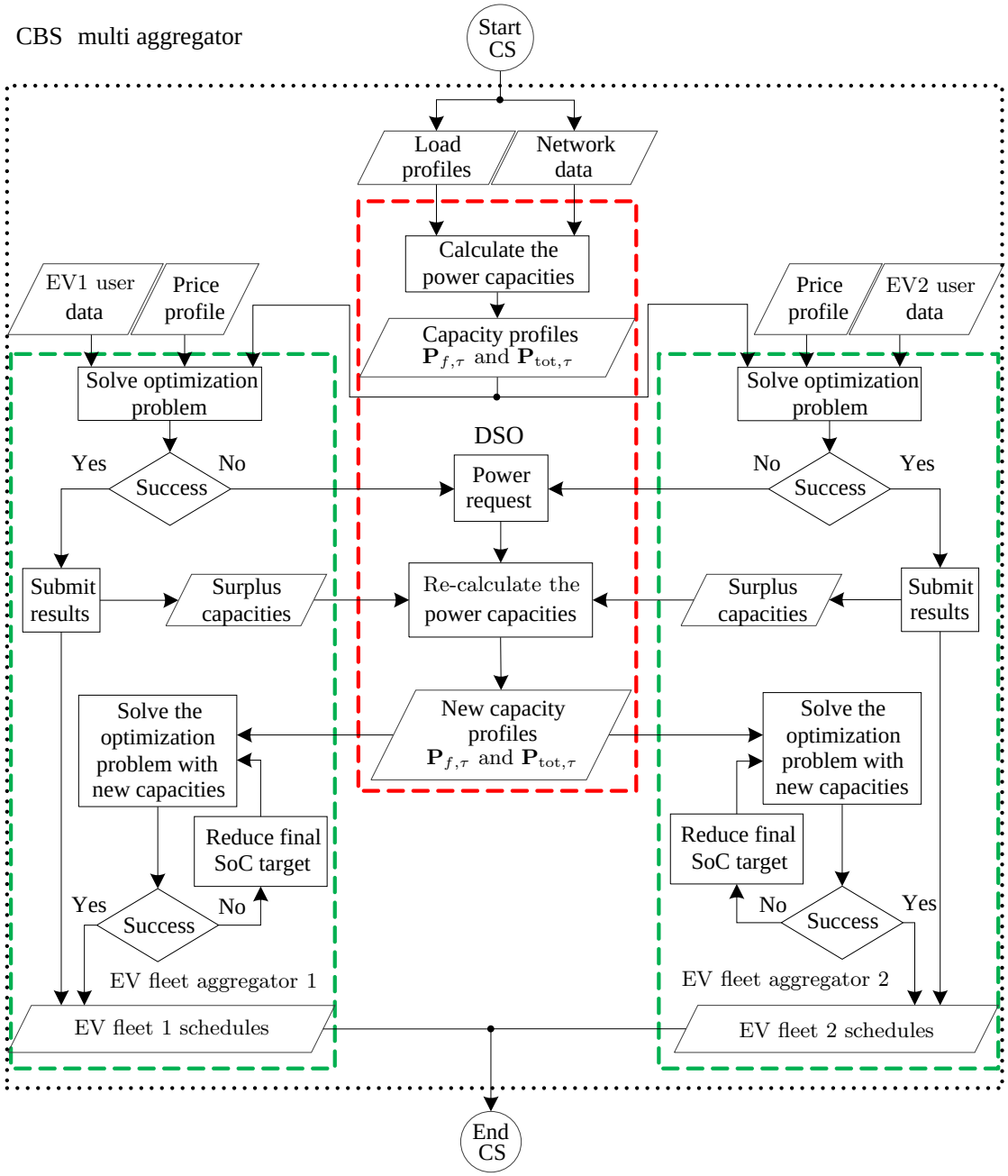

Figure 27: Detailed Flowchart for Two Aggregator Scheme

Appendix C

EV Model Validation

In this part, the used EV charging model, introduced in section 3.2 is tuned to reflect the charging behavior of Mitsubishi iMiEV.

C.1 Data

For the validation work, the iMiEV data-sheet [44] donates the needed specifications for the battery model and the on-board charger. The used measurement data for the specific EV battery and charger behavior is attained from the project: „Integrierte Tests der (Fahr-) und Ladeeigenschaften von Elektrofahrzeugen“ conducted by Dipl.-Ing. Johannes Prior at Fraunhofer IWES, Kassel. To simulate the individual battery cell, the data from [52] is used. The publication presents detailed measurement results for the „LEV50“ type battery cells, which are also used in Mitsubishi iMiEV. This data is used to find the coefficient values for the on-board charger, for the battery resistance and for the battery inner voltage source. Dr. Frank Marten from Fraunhofer Iwes, Kassel preformed the earlier battery validation work and his methods and documentation are used as a basis for the validation of the EV charging model.

C.2 Methods

The charger logic block and the battery model block, introduced in section 3.2, were developed to represent the dynamic and complex behavior of a real EV. In the used EV model, the charger is mathematically modeled by using the 2nd order polynomial function introduced by [53]. This function is formulated as:

$$P_{\mathrm{DC}} = -\alpha_1 + (1 - \alpha_2) \cdot P_{\mathrm{AC}} - \alpha_3 \cdot {P_{\mathrm{AC}}}^2, \tag{C.2.1}$$

where the DC power P_{DC} is calculated by considering the AC power P_{AC} as a variable. The α_1, α_2 and α_3 are the loss coefficients. The measurement data for AC charging power between a range of 0.63 kW to 3.2 kW is used to calculate the charger's AC-DC power conversion losses. These values define the 2nd order polynomial function, which is shown above. This is done in similar manner as in Figure 30.

A simplified model of a charger and a battery is presented in Figure 28. The battery is modeled as a circuit with a DC voltage source and a resistor connected in series. They are both variable depending on the battery SoC. The current integration method is used in this EV model to determine the SoC and it can be defined as:

$$SoC = \int \frac{I_{\mathrm{DC}}}{\beta \mathrm{batt}} dt, \tag{C.2.2}$$

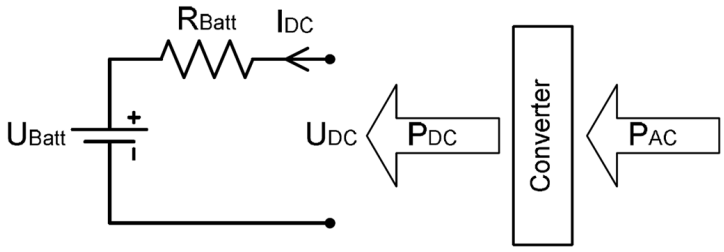

Figure 28: Schematic diagram of the EV charger and battery [10].

where the DC current I_{DC} is accumulated over time in relation to the battery capacity βbatt which is measured in ampere-hours [Ah]. The received SoC value is used in the charging logic block to calculate the battery DC voltage with a 2nd order polynomial function and it can presented as follows:

$$U_{\mathrm{batt}} = \xi \cdot \left(\zeta_1 + \zeta_2 \cdot SoC + \zeta_3 \cdot SoC^2\right), \tag{C.2.3}$$

where U_{batt} is the internal battery voltage, ξ is the number of cells in series in the battery and ζ_1, ζ_2 and ζ_3 are the voltage coefficients. The battery's inner resistance is defined in the charging logic by a 6th order polynomial function which is:

$$R_{\mathrm{batt}} = \left(\frac{\xi}{\rho}\right) \cdot \begin{pmatrix} \eta_1 + \eta_2 \cdot SoC + \eta_3 \cdot SoC^2 + \eta_4 \cdot SoC^3 \\ + \eta_5 \cdot SoC^4 + \eta_6 \cdot SoC^5 + \eta_7 \cdot SoC^6 \end{pmatrix}, \tag{C.2.4}$$

where R_{batt} is the internal resistance of the battery, ρ is the number of cells in parallel in the battery and $\eta_1 - \eta_7$ are the resistance coefficients. To tune the coefficients in equations (C.2.3) and (C.2.4), the behavior of a single battery cell needs to be replicated. To obtain the behavior of a single battery cell, the discharging behavior of LEV50 cell on different discharging currents, presented in Figure 29, is used.

The voltage values are visually estimated to calculate the resistance and the voltage averages, as presented in Table C.1. The resistance differences are calculated according to different discharge currents as illustrated in Table C.1. From these resistance differences, the average values are taken as function of SoC. Accordingly the resistance coefficient values $\eta_1 - \eta_7$ are formulated. To calculate the voltage coefficient, the open circuit voltages are calculated for the corresponding battery SoC rates. For this the summation of the estimated voltage and the voltage calculated by the average resistance and the corresponding current is used. Accordingly average open voltages are calculated for the corresponding SoC rates. Moreover, curve fitting, illustrated in Figure 30, is used to determine the 2nd order polynomials for the voltage coefficients $\zeta_1 - \zeta_3$.

The values obtained by the calculations are nearly the same as the ones Dr. Marten had in his validation work. Dr. Marten also mentioned in his work that

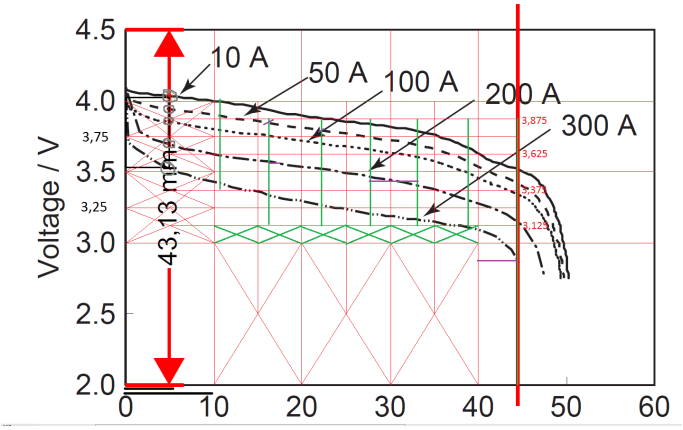

Figure 29: LEV50 cell voltage values with different discharge currents [52].

Table C.1: Battery efficiency calculations

SOC	Cap (Ah)	V @ 0,5xC	V @ 2xC	V @ 3xC	R @ 0,5-2	R @ 0,5 - 3	R @ 2 - 3	R ave	Voc @ 0,5xC	Voc @ 2xC	Voc @ 3xC	Voc ave
0.876	5.6	3.95	3.69	3.49	0.0017	0.0018	0.0020	0.0019	4.04	4.06	4.05	4.05
0.753	11.1	3.90	3.62	3.43	0.0019	0.0019	0.0019	0.0019	3.99	4.00	3.99	4.00
0.629	16.7	3.84	3.57	3.32	0.0018	0.0021	0.0025	0.0021	3.95	4.00	3.96	3.97
0.504	22.3	3.80	3.51	3.28	0.0019	0.0021	0.0023	0.0021	3.91	3.93	3.91	3.92
0.382	27.8	3.74	3.45	3.19	0.0019	0.0022	0.0026	0.0022	3.85	3.90	3.86	3.87
0.264	33.11	3.69	3.40	3.16	0.0019	0.0021	0.0024	0.0022	3.80	3.83	3.81	3.81
0.146	38.42	3.56	3.30	3.11	0.0017	0.0018	0.0019	0.0018	3.65	3.66	3.65	3.66
0.025	43.87	3.43	3.16	2.87	0.0018	0.0022	0.0029	0.0023	3.55	3.62	3.56	3.58
Currents		50	200	300								

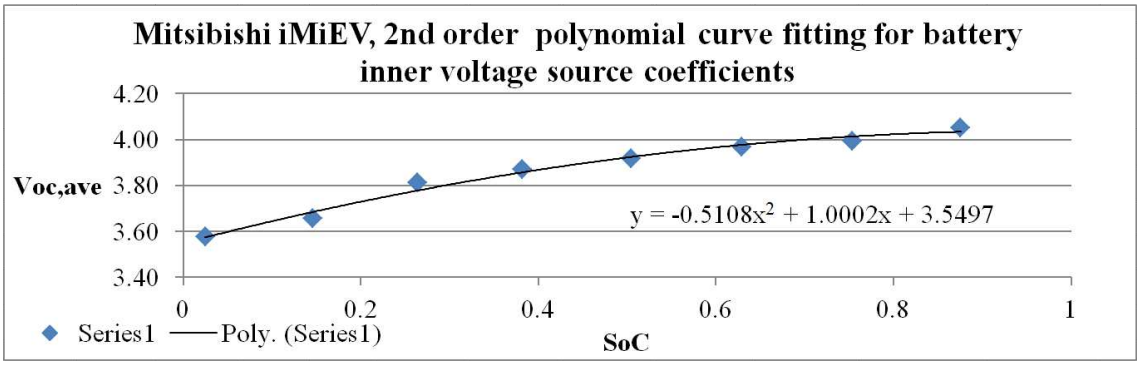

Figure 30: Battery inner voltage source coefficients by a 2nd order polynomial curve fitting

even tough one single cell is well modeled it cannot be multiplied to present a complete battery pack. The battery pack, consisting of multiple individual cells, has its own characteristics, due to the fact that the cells are not perfectly identical. Therefore, it is necessary to determine a scaling factor in order to better reproduce

the accumulated behavior of the cells as a whole.

C.3 Parameter Fitting and Correction Factors

The battery capacity decreases as the battery ages. Paper [54] shows that the Li-ion battery degradation can be linearly estimated till a certain degree as illustrated in Figure 31. Authors in [54] also describe that the cell voltages start to drop in an almost uniform way as the number of loading cycles increases. Some degradation also occurs when the battery is kept without usage. The cell resistance increases uniformly with different DoD percentages.

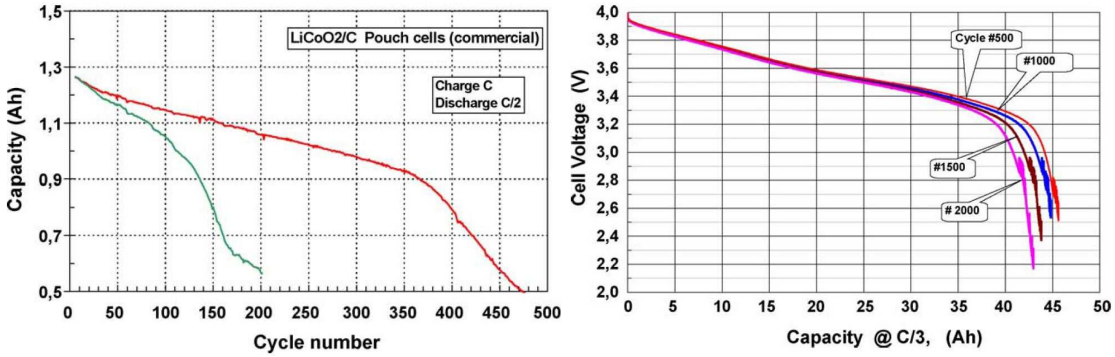

Figure 31: Battery degradation as a function of the loading cycles [54].

For example, if the battery has already 1000 charging cycles, the end capacity drops with around 1,11 Ah compared to a battery which has only 500 charging cycles. Motivated by [54], a correction factor for the battery capacity is additionally implemented within the range of 27-45 Ah in order to model the degradation effect of the battery. Therefore only the corresponding values, presented in Table C.1, from the chosen range need to be altered stepwise. As the amount of loading cycles is not known, an alternative approach is used. The battery degradation can also be estimated by substituting the realized charging capacity from the new battery's maximum charging capacity. Even though the capacity of a new battery is 50 Ah, it is assumed that the charger has an internal SoC limit to charge the battery only until it reaches 90% SoC. Therefore, the real used capacity is only 45 Ah.

The realized charging capacity can be calculated by taking the battery's maximum DC energy and dividing it by the battery's maximum DC voltage. The realized charging capacity is 44,437 Ah, which after substituting results in a battery degradation of 0,563 Ah. As the charger parameters also influence the outcomes, it is seen that the real charger is working at lower efficiency. Therefore a correction factor is also added to the charger function. The measured DC power values are uniformly multiplied by the correction factor, so that the new coefficient polynomials are calculated more accurately. Moreover, The li-ion battery has two charging periods in its charging process, which are namely constant power and constant voltage charging. The turning point of these two periods is defined by the maximum DC voltage of the battery. To fit the turning point of the constant voltage charging and the constant power charging range, correction factors are applied separately to the voltage

and the resistance characteristics. These two factors are used to multiply the mean resistance and voltage values accordingly. The multiplied mean values are used to calculate the new η and the ζ for the battery model.

C.4 Results

For model validation, the measured AC voltage is used in the developed EV model as an input. Output of the model, battery DC voltage, battery DC current and the DC charging power are compared with the measurement data. To determine the different correction factors which represent the non-ideal behavior of the measured battery, the tuning process is done iteratively till it reaches a reasonable maximum error. The original measurement data as well as the simulations resolution is chosen as 1 second, but in order to mitigate the measurement noise, both of them are scaled to 1 min resolution. As this does not entirely address the issue of highly fluctuating measurement data, the end part of the charging process is ruled out from the error calculation. The part used for error calculations starts from 35 min and ends at 328 min. The validation results are shown in Figure 32.

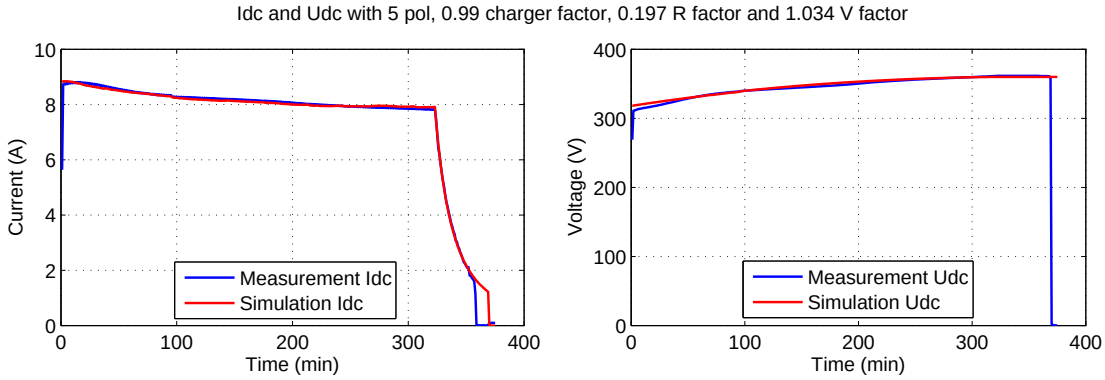

Figure 32: Comparison of DC currents and voltages

The maximum relative error between the simulated and measured direct current is 2,1% and for the voltage it is 1,0%. The parameters received from this tuning work are implemented in the EV model to define the charging behavior.

Appendix D

Penalty Factor's Influence to the Primary Objective Function

The penalty factors C_P and P_P are studied to enhance the charging scheduling decision making process. These penalty factors are used in the cost minimization objective function (2.2.1) and in the valley filling and load shifting objective function (2.3.1) introduced in chapter 2. Small C_P and P_P cause the secondary objective to lose its worth and the charging of one specific EV to happen with multiple interruptions. However, too large factors cause the solver to ignore the primary objective function. To search proper values for these penalty factors, the ABS, DBS and the SBS are used. Next, the data and methods are introduced. Subsequently the case study and results are presented. Lastly, recommended solutions are provided.

D.1 Data and Methods

A trial and error method is used to map the region where both of the objective functions are noticed by the solver and a more accurate study can be conducted. The used data and the simulation environment are introduced in chapter 3. To simplify and speed up the study, the EV model and grid simulations are bypassed. The EV battery behavior is replicated with simple calculations. The simulation step is 30 minutes and the optimization horizon is 14 hours. The used EV penetration rate is 50%.

D.2 Results

The results are analyzed in terms of the apparent efficiency degradation in the primary objective function and the amount of interruptions in the whole EV fleet charging. The ABS and SBS results are evaluated based on charging cost changes as the C_P increases and on the number of interruptions in the EV charging. The DBS results are evaluated based on the changes in the cumulative peak power cP_EV, occurring due to EV charging as the P_P increases and on the number of interruptions in the EV charging.

First, the C_P in the ABS is chosen for inspection. The numerical results are gathered in Table D.1 and for comparison, a scenario where the $C_\mathrm{P} = 0$ is also presented. Here a variable step size is used in order to narrow down the amount of simulation.

The Inter. in Table D.2 describes the total number of charging interruptions in the charging of the whole EV fleet. Here, cost is the total charging cost of the EV fleet in Euros (€). The zero case presents the largest amount of interrupted charging incidences and the largest C_P leads to a situation where all of the EVs are charged

Table D.1: The C_{P} influence in the ABS

C_{P}	0	0.01	0.025	0.04	0.055	0.07	0.08	0.11	0.14	0.17	0.20
Inter.	64	47	15	3	0	0	0	0	0	0	0
Cost [€]	12.3	12.0	12.5	13.2	13.9	13.9	14.3	14.3	14.3	14.3	14.3

in a continuous manner. From these results it can be seen that for the specific day and EV penetration rate considered, the $C_{\mathrm{P}} = 0.055$ could be chosen as it results in zero interruptions and the total charging cost is only 16% higher compared to $C_{\mathrm{P}} = 0.01$. Next, the SBS is studied with the same C_{P} region as the ABS. The results are presented in Table D.2.

Table D.2: The C_{P} influence in the SBS

C_{P}	0	0.01	0.025	0.04	0.055	0.07	0.08	0.11	0.14	0.17	0.20
Inter.	64	29	10	4	2	2	1	0	0	0	1
Cost [€]	13.2	13.4	13.9	14.3	14.7	14.7	14.8	15.0	15.0	15.1	15.1

Here the results follow the same pattern as in the ABS case, except that the largest C_{P} differs from its predecessors. It shows that one interruption occurs in the charging. This can be explained by the nature of the optimization process and the more constrained optimization problem the SBS presents. The results shows that the first zero interruption case could be found at $C_{\mathrm{P}} = 0.11$ and at this value the total charging cost is only 14% higher compared to the minimum cost case at $C_{\mathrm{P}} = 0$.

Finally, the DBS and P_{P} are taken into inspection. The suitable region for study is between $P_{\mathrm{P}} = 0.001$ and $P_{\mathrm{P}} = 0.01$, with 0.001 steps. The results for the DBS and P_{P} are gathered in Table D.3.

Table D.3: The P_{P} influence in the DBS

$P_{\mathrm{P}} \cdot 10e-4$	0	1	2	3	4	5	6	7	8	9	10
Inter.	59	21	8	4	3	3	2	1	1	1	0
$\mathrm{cP_{EV}}$ [kVA]	128	108	114	110	118	114	126	130	130	141	137

In Table D.3, the $\mathrm{cP_{EV}}$ is the maximum load of the aggregated load profile representing the loading at the distribution transformer when the EVs are in charging. The number of interruptions decreases rapidly till 3 but after this the P_{P} needs to increase till 0,01 before the solver is willing to charge all of the EVs without interruptions. Meanwhile, the $\mathrm{cP_{EV}}$ value is increasing roughly 25% from minimum case at $P_{\mathrm{P}} = 0.001$ till the zero case at $P_{\mathrm{P}} = 0.01$. After $P_{\mathrm{P}} = 0.005$, the $\mathrm{cP_{EV}}$ begins to increase considerably, which indicates that the primary objective is becoming insignificant. To understand these changes better, the results are also inspected visually from the charts presented in Figure 33.

In Figure 33 it can be observed that for $P_{\mathrm{P}} = 0.01$, the primary objective is starting to suffer considerably. The $P_{\mathrm{P}} = 0.005$ shows only small change in the

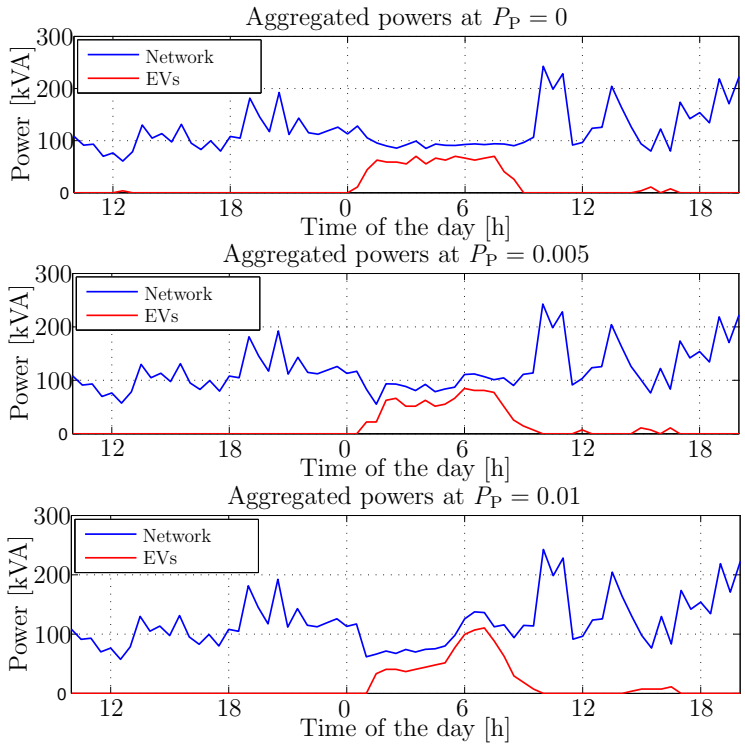

Figure 33: Aggregated powers by the DBS with different P_P

cumulative charging profile. However, the results are assumed to be different when the used price profile or the EV behavior changes. To account for these changes, more exhaustive studies would be needed. However, as the focus of this work is not in parameter optimization the attained results are considered to be satisfactory.

D.3 Recommendations

Based on this study, a C_P of 0.1 is proposed to be used in the cost minimization objective function (2.2.1). This value is a compromise value, by which close to zero interruption can be assumed by both of the used strategies and the total charging increment can be considered reasonable. A P_P value of 0.005 represents a suitable compromise value for the DBS and the valley filling and load shifting objective function (2.3.1). As the DBS is more electric network oriented, 3 interruptions in the whole EV fleet charging can be considered acceptable. With this penalty factor, the primary objective function of the DBS is still working sufficiently because the cP_{EV} increased only by 6% compared to the minimum case. It is to be noted that these suggested penalty factors are tuned for 30 minute simulation step and the values for different simulation steps need to be multiplied with corresponding factors. E.g. for 60 minute simulation intervals, the factors should be doubled and for 15 minute intervals they should be halved.

Appendix E

Simulation Results

Table E.1: Wednesday, Multi aggregator results 1 with 75% EV penetration rate

Wednesday, Aggregator 1 with 30% share of EVs on 75% EV penetration rate					
Combination:	UCS-CBS	ABS-CBS	DBS-CBS	SBS-CBS	CBS-CBS
Total cost [€]	44.3	24.1	32.1	25.9	24.7
Cost change [%]	-48.3	-71.8	-62.6	-69.7	-71.2
Net interrupt.	-12	-13	15	-11	-12
Flexibility [h]	6	3	3	3	3
Min SoC	0.9	0.9	0.9	0.9	0.9
Max load [kVA]	287	302	287	287	287
Max current [A]	331.1	304.4	257.2	262.8	264.7
Viol. magn. [%]	16.6	7.2	0.0	0.0	0.0
Viol. dur. [min]	1	2	0	0	0
Loss change [%]	-30.9	-27.7	-40.0	-32.0	-28.9
Cost of losses [€]	3.4	1.5	1.6	1.6	1.6

Wednesday, Aggregator 1 with 50% share of EVs on 75% EV penetration rate					
Combination:	UCS-CBS	ABS-CBS	DBS-CBS	SBS-CBS	CBS-CBS
Total cost [€]	55.3	24.1	38.9	26.0	24.9
Cost change [%]	-35.4	-71.9	-54.6	-69.6	-70.9
Net interrupt.	-10	-12	30	-1	-14
Flexibility [h]	8	3	2	3	3
Min SoC	0.9	0.9	0.9	0.9	0.9
Max load [kVA]	301	341	287	287	287
Max current [A]	331.4	304.4	270.1	257.2	281.7
Viol. magn. [%]	16.7	7.2	0.0	0.0	0.0
Viol. dur. [min]	1	2	0	0	0
Loss change [%]	-28.1	-27.1	-46.1	-32.6	-29.5
Cost of losses [€]	4.3	1.5	1.7	1.6	1.6

Table E.2: Wednesday, Multi aggregator results 2 with 75% EV penetration rate

Wednesday, Aggregator 1 with 70% share of EVs on 75% EV penetration rate					
Combination:	UCS-CBS	ABS-CBS	DBS-CBS	SBS-CBS	CBS-CBS
Total cost [€]	67.0	23.9	46.9	26.2	24.8
Cost change [%]	-21.8	-72.1	-45.2	-69.5	-71.0
Net interrupt.	-8	-12	53	5	-8
Flexibility [h]	9	3	2	3	3
Min SoC	0.9	0.9	0.9	0.9	0.9
Max load [kVA]	320	372	287	287	287
Max current [A]	331.4	360.8	270.1	275.1	287.6
Viol. magn. [%]	16.7	27.0	0.0	0.0	1.3
Viol. dur. [min]	1	27	0	0	1
Loss change [%]	-21.2	-24.8	-49.8	-33.5	-28.9
Cost of losses [€]	5.7	1.5	2.1	1.6	1.6

Wednesday, Aggregator 1 with 100% share of EVs on 75% EV penetration rate					
Combination:	UCS-CBS	ABS-CBS	DBS-CBS	SBS-CBS	CBS-CBS
Total cost [€]	85.7	23.2	59.6	28.2	24.7
Cost change [%]	0.0	-73.0	-30.4	-67.1	-71.2
Net interrupt.	0	-13	79	16	-3
Flexibility [h]	12	3	2	3	3
Min SoC	0.9	0.9	0.9	0.9	0.9
Max load [kVA]	346	427	287	287	287
Max current [A]	347.5	440.8	256.5	249.5	287.6
Viol. magn. [%]	22.4	55.2	0.0	0.0	1.3
Viol. dur. [min]	8	32	0	0	1
Loss change [%]	0.0	-19.6	-50.0	-35.3	-27.3
Cost of losses [€]	8.0	1.6	3.1	1.6	1.6

Table E.3: Wednesday, Multi aggregator results 1 with 100% EV penetration rate

Wednesday, Aggregator 1 with 30% share of EVs on 100% EV penetration rate					
Combination:	UCS-CBS	ABS-CBS	DBS-CBS	SBS-CBS	CBS-CBS
Total cost [€]	56.8	32.1	42.9	37.0	33.4
Cost change [%]	-46.0	-69.5	-59.2	-64.8	-68.2
Net interrupt.	12	6	42	22	17
Flexibility [h]	6	3	3	3	3
Min SoC	0.9	0.9	0.9	0.9	0.9
Max load [kVA]	287	354	287	287	287
Max current [A]	299.6	342.4	282.8	280.6	271.6
Viol. magn. [%]	5.5	20.6	0.0	0.0	0.0
Viol. dur. [min]	1	27	0	0	0
Loss change [%]	-32.4	-21.7	-36.8	-31.2	-26.1
Cost of losses [€]	3.9	2.1	2.2	2.2	2.2

Wednesday, Aggregator 1 with 50% share of EVs on 100% EV penetration rate					
Combination:	UCS-CBS	ABS-CBS	DBS-CBS	SBS-CBS	CBS-CBS
Total cost [€]	69.4	31.5	53.9	37.6	33.9
Cost change [%]	-34.0	-70.0	-48.7	-64.3	-67.8
Net interrupt.	0	-6	48	18	-5
Flexibility [h]	8	3	2	3	3
Min SoC	0.9	0.9	0.9	0.9	0.9
Max load [kVA]	298	394	287	287	287
Max current [A]	347.9	390.5	259.8	259.8	271.6
Viol. magn. [%]	22.5	37.5	0.0	0.0	0.0
Viol. dur. [min]	2	33	0	0	0
Loss change [%]	-29.1	-19.1	-42.9	-31.0	-27.0
Cost of losses [€]	5.2	2.1	2.6	2.3	2.2

Table E.4: Wednesday, Multi aggregator results 2 with 100% EV penetration rate

Wednesday, Aggregator 1 with 70% share of EVs on 100% EV penetration rate					
Combination:	UCS-CBS	ABS-CBS	DBS-CBS	SBS-CBS	CBS-CBS
Total cost [€]	83.2	30.8	59.6	38.3	34.4
Cost change [%]	-20.8	-70.7	-43.3	-63.6	-67.3
Net interrupt.	-2	-8	71	36	11
Flexibility [h]	10	3	3	3	4
Min SoC	0.9	0.9	0.9	0.9	0.9
Max load [kVA]	316	444	287	287	287
Max current [A]	364.0	484.3	266.1	267.2	271.6
Viol. magn. [%]	28.2	70.5	0.0	0.0	0.0
Viol. dur. [min]	3	49	0	0	0
Loss change [%]	-21.6	-15.8	-44.0	-33.3	-27.3
Cost of losses [€]	6.8	2.1	3.0	2.3	2.2

Wednesday, Aggregator 1 with 100% share of EVs on 100% EV penetration rate					
Combination:	UCS-CBS	ABS-CBS	DBS-CBS	SBS-CBS	CBS-CBS
Total cost [€]	105.1	28.5	67.3	41.5	34.1
Cost change [%]	0.0	-72.9	-36.0	-60.5	-67.6
Net interrupt.	0	-15	110	49	15
Flexibility [h]	12	3	2	4	4
Min SoC	0.9	0.9	0.9	0.9	0.9
Max load [kVA]	353	538	287	287	287
Max current [A]	396.2	548.5	285.0	283.4	292.9
Viol. magn. [%]	39.5	93.1	0.4	0.0	3.1
Viol. dur. [min]	12	49	1	0	1
Loss change [%]	0.0	-3.7	-40.3	-33.9	-25.6
Cost of losses [€]	9.6	2.2	3.7	2.4	2.2

Table E.5: Saturday, Multi aggregator results 1 with 75% EV penetration rate

Saturday, Aggregator 1 with 30% share of EVs on 75% EV penetration rate					
Combination:	UCS-CBS	ABS-CBS	DBS-CBS	SBS-CBS	CBS-CBS
Total cost [€]	23.8	15.1	17.9	15.1	14.9
Cost change [%]	-41.5	-62.9	-55.9	-62.9	-63.3
Net interrupt.	-8	-15	12	-15	-13
Flexibility [h]	9	6	5	5	5
Min SoC	0.9	0.9	0.9	0.9	0.9
Max load [kVA]	282	267	267	267	267
Max current [A]	298.2	266.7	186.6	234.7	224.6
Viol. magn. [%]	5.0	0.0	0.0	0.0	0.0
Viol. dur. [min]	1	0	0	0	0
Loss change [%]	-25.4	-15.8	-37.4	-21.0	-22.3
Cost of losses [€]	1.3	0.8	0.7	0.8	0.8

Saturday, Aggregator 1 with 50% share of EVs on 75% EV penetration rate					
Combination:	UCS-CBS	ABS-CBS	DBS-CBS	SBS-CBS	CBS-CBS
Total cost [€]	29.5	14.4	20.1	15.4	14.5
Cost change [%]	-27.5	-64.6	-50.6	-62.1	-64.2
Net interrupt.	-7	-16	21	-18	-12
Flexibility [h]	11	5	4	5	4
Min SoC	0.9	0.9	0.9	0.9	0.9
Max load [kVA]	301	276	267	267	267
Max current [A]	307.5	275.2	188.1	211.2	253.8
Viol. magn. [%]	8.3	0.0	0.0	0.0	0.0
Viol. dur. [min]	1	0	0	0	0
Loss change [%]	-18.9	-13.5	-39.7	-27.3	-19.8
Cost of losses [€]	1.8	0.8	0.8	0.7	0.7

Table E.6: Saturday, Multi aggregator results 2 with 75% EV penetration rate

Saturday, Aggregator 1 with 70% share of EVs on 75% EV penetration rate					
Combination:	UCS-CBS	ABS-CBS	DBS-CBS	SBS-CBS	CBS-CBS
Total cost [€]	32.8	14.3	22.4	15.4	15.1
Cost change [%]	-19.4	-64.7	-44.9	-62.2	-62.9
Net interrupt.	-6	-18	36	-18	-17
Flexibility [h]	14	4	4	5	5
Min SoC	0.9	0.9	0.9	0.9	0.9
Max load [kVA]	301	268	267	267	267
Max current [A]	314.3	259.2	237.4	222.4	240.4
Viol. magn. [%]	10.7	0.0	0.0	0.0	0.0
Viol. dur. [min]	1	0	0	0	0
Loss change [%]	-17.0	-14.6	-39.4	-22.8	-18.6
Cost of losses [€]	2.0	0.8	0.9	0.8	0.8

Saturday, Aggregator 1 with 100% share of EVs on 75% EV penetration rate					
Combination:	UCS-CBS	ABS-CBS	DBS-CBS	SBS-CBS	CBS-CBS
Total cost [€]	40.6	14.3	26.6	16.0	15.2
Cost change [%]	0.0	-64.8	-34.6	-60.7	-62.6
Net interrupt.	0	-18	43	-13	-15
Flexibility [h]	18	4	5	6	5
Min SoC	0.9	0.9	0.9	0.9	0.9
Max load [kVA]	308	288	267	267	267
Max current [A]	323.9	307.2	216.4	207.3	250.7
Viol. magn. [%]	14.1	8.2	0.0	0.0	0.0
Viol. dur. [min]	1	26	0	0	0
Loss change [%]	0.0	-11.7	-44.8	-28.8	-20.1
Cost of losses [€]	2.7	0.8	1.0	0.7	0.8

Table E.7: Saturday, Multi aggregator results 1 with 100% EV penetration rate

Saturday, Aggregator 1 with 30% share of EVs on 100% EV penetration rate					
Combination:	UCS-CBS	ABS-CBS	DBS-CBS	SBS-CBS	CBS-CBS
Total cost [€]	36.0	25.6	29.3	26.7	25.9
Cost change [%]	-41.2	-58.2	-52.1	-56.3	-57.6
Net interrupt.	-3	-13	17	-13	-15
Flexibility [h]	10	6	6	6	6
Min SoC	0.9	0.9	0.9	0.9	0.9
Max load [kVA]	286	291	267	267	267
Max current [A]	282.0	288.6	240.1	224.6	227.5
Viol. magn. [%]	0.0	1.6	0.0	0.0	0.0
Viol. dur. [min]	0	2	0	0	0
Loss change [%]	-31.7	-20.3	-33.5	-28.4	-25.2
Cost of losses [€]	1.9	1.5	1.4	1.4	1.4

Saturday, Aggregator 1 with 50% share of EVs on 100% EV penetration rate					
Combination:	UCS-CBS	ABS-CBS	DBS-CBS	SBS-CBS	CBS-CBS
Total cost [€]	42.4	25.3	33.3	27.1	26.3
Cost change [%]	-30.6	-58.7	-45.5	-55.7	-57.0
Net interrupt.	-6	-19	26	-14	-14
Flexibility [h]	12	6	5	6	6
Min SoC	0.9	0.9	0.9	0.9	0.9
Max load [kVA]	301	321	267	267	267
Max current [A]	298.2	307.2	226.2	209.2	232.3
Viol. magn. [%]	5.0	8.2	0.0	0.0	0.0
Viol. dur. [min]	1	28	0	0	0
Loss change [%]	-30.6	-19.7	-39.8	-30.1	-26.0
Cost of losses [€]	2.4	1.4	1.4	1.4	1.4

Table E.8: Saturday, Multi aggregator results 2 with 100% EV penetration rate

Saturday, Aggregator 1 with 70% share of EVs on 100% EV penetration rate					
Combination:	UCS-CBS	ABS-CBS	DBS-CBS	SBS-CBS	CBS-CBS
Total cost [€]	50.7	25.4	35.5	27.5	26.0
Cost change [%]	-17.0	-58.5	-41.8	-55.0	-57.4
Net interrupt.	-5	-24	50	-3	-1
Flexibility [h]	14	6	6	6	6
Min SoC	0.9	0.9	0.9	0.9	0.9
Max load [kVA]	319	339	267	267	267
Max current [A]	341.9	350.8	268.7	240.2	258.0
Viol. magn. [%]	20.4	23.5	0.0	0.0	0.0
Viol. dur. [min]	3	46	0	0	0
Loss change [%]	-26.2	-12.5	-34.4	-29.7	-25.7
Cost of losses [€]	3.0	1.5	1.7	1.4	1.4

Saturday, Aggregator 1 with 100% share of EVs on 100% EV penetration rate					
Combination:	UCS-CBS	ABS-CBS	DBS-CBS	SBS-CBS	CBS-CBS
Total cost [€]	61.1	26.7	43.7	29.2	26.9
Cost change [%]	0.0	-56.3	-28.5	-52.2	-55.9
Net interrupt.	0	-20	86	9	-1
Flexibility [h]	18	7	6	7	6
Min SoC	0.9	0.9	0.9	0.9	0.9
Max load [kVA]	356	311	267	267	267
Max current [A]	374.3	323.2	274.5	233.8	272.5
Viol. magn. [%]	31.8	13.8	0.0	0.0	0.0
Viol. dur. [min]	5	48	0	0	0
Loss change [%]	0.0	-8.9	-36.4	-32.4	-25.6
Cost of losses [€]	4.6	1.8	2.2	1.5	1.5